Validation of the Shallow Landslide Model, SHALSTAB, for Forest Management

William E. Dietrich and Dino Bellugi

Department of Earth and Planetary Science, University of California, Berkeley

Raphael Real de Asua

Stillwater Sciences, Berkeley, California

There are increasing demands at the regional, watershed and local level to reduce the incidence of shallow landsliding resulting from forest management practices. Here we report a validation study of SHALSTAB, a simple mechanistic model for delineating the relative potential for shallow landsliding across the landscape. The cohesionless, infinite-slope model a uses topographically-driven, steady-state shallow subsurface flow theory to estimate the spatial distribution of destabilizing pore pressure. The calculated ratio of the effective precipitation, q, to the soil transmissivity, T at instability is used to map the relative potential for landsliding. We assume that sites with the same q/T value have the same relative potential for instability, and sites with the lowest q/T are least stable. Potential instability (i.e. q/T) is dominated by the drainage area per cell size rather than hillslope gradient for slopes between 20 and 40 degrees. We validated the model (using fixed parameters) in 7 watersheds in Northern California by comparing the frequency of shallow landslides per unit area of q/T classes with that produced using a biased random-placement model of similar sized landslide scars. Over 1100 landslides were mapped and comparisons suggest that for a 10 m grid, a log(q/T) threshold of less than –2.8 covers about 13% of the watershed and predicts on average about 60% of the shallow landslide locations. Hence, the model can discriminate a relatively small part of the landscape that produces the majority of shallow landslides. Model performance depends strongly on the quality of the topographic base map; 10 m grid data derived from USGS 7.5' topographic maps miss important fine-scale topography. This study suggests that SHALSTAB may be useful in regional planning, watershed analyses and timber harvest planning. For site-specific land management practices, field surveys are needed to evaluate the accuracy of the topographic maps and as well other factors affecting local slope stability.

INTRODUCTION

In the steep, forested coastal mountains of the Pacific Northwest, shallow landslides are a major source of sediment delivered to streams (Figure 1). Individual landslides may mobilize into debris flows, and travel downstream

Land Use and Watersheds: Human Influence on Hydrology and Geomorphology in Urban and Forest Areas
Water Science and Application Volume 2, pages 195-227
Copyright 2001 by the American Geophysical Union

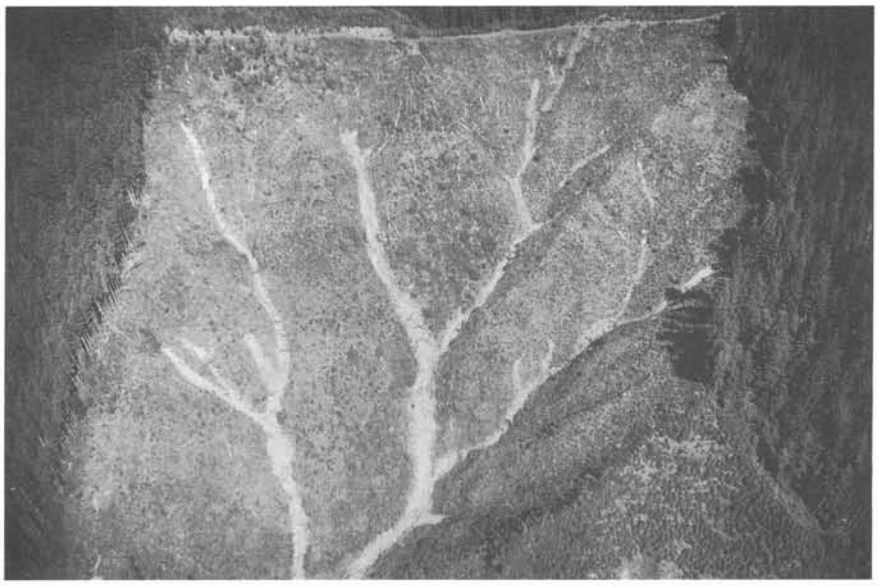

Figure 1. Debris flow scars resulting from 1996 storms in the Oregon Coast Range. Note that the scars are originating in the hollows lying at the tips of the valley network. Photograph by John Stock.

scouring channels of all sediment and wood, then depositing the acquired mass in a large accumulation where the flow comes to rest [e.g. Dietrich and Dunne, 1978; Hungr et al., 1984; Benda and Dunne, 1997]. Although shallow landsliding and associated debris flows are an integral part of natural geomorphic processes, forest management practices can greatly increase the frequency of their occurrence [e.g. Sidle et al., 1985], which can lead to degradation of stream habitat and loss of habitat features either through scour to bedrock or high sediment loading. Where people live in areas adjacent to lands managed for timber production, there is also an increased chance of forest management actions triggering landslides that pose a risk to human life and property.

As part of landscape-level land use planning efforts mandated by various recent state and federal regulations in the United States, forest managers have been seeking ways to delineate shallow landslide potential on their lands in order to develop management prescriptions that minimize increases in slope instability while sustaining timber harvesting goals. Typically such landslide potential maps must be generated with limited information: geologic, topographic and land use maps and limited aerial photograph coverage. Such things as soil strength, root strength dynamics, and site hydrologic characteristics, all of which strongly influence slope stability are normally not known quantitatively. These properties can vary significantly on spatial scales of only a few meters, making their systematic mapping a daunting task. We are aware of no such spatially registered information in the Pacific Northwest. In response to this absence of data we have explored the use of a simple, mechanistic model for shallow slope stability (typically involving just the soil mantle) [Dietrich et al., 1992, 1993; Montgomery and Dietrich, 1994; Dietrich and Sitar, 1997; Dietrich and Montgomery, 1998, Dietrich et al., 1998]. We suggest that this model, now turned into the computer model SHALSTAB (available at http://socrates.berkeley.edu/~geomorph/), is perhaps the simplest, process-based model that accounts for the topographic control on pore pressure development responsible for shallow slope instability. Federal and state agencies as well as private companies are increasingly using this model. Here we review the basic theory for the model, illustrate how it can be validated and applied in various contexts, and discuss important issues of interpretation and further developments of the model. A central issue here is that SHALSTAB (or any such digital terrain model) is only as good as the available topographic data. In areas with adequate topographic data, we have found that mapped landslides preferentially occur in areas predicted by SHALSTAB to be most prone to slope instability.

PREVIOUS WORK

Montgomery and Dietrich [1994] briefly review the general approaches that have been taken to assessing land-

slide hazards. These approaches range from field mapping and intuitive extrapolation to multivariate analysis and to mechanistic-based theory. At least four different approaches have been explored in forest management applications.

One approach involves creating a map of observed shallow landslides based on interpretation of aerial photographs and field inspections, using professional judgment and knowledge of local geology and topography to classify the land into landslide hazard categories, and then specifying the types of management that can be conducted in these areas (no road construction, selective harvest, etc.). This is the approach taken in most watershed analyses that follow the Washington State Department of Natural Resources methodology for watershed analysis [WFPB, 1997]. The strength of this approach is that it is based on field investigations, and if the mapper has adequate knowledge of factors influencing landslide processes, reliable interpretations may often be obtained. Its weakness is that landslide maps only reveal where landslides have occurred, not where they are most likely to occur in the future. Hence, the mapmaker must rely on intuition and experience to estimate the full extent of landslide potential existing in a watershed. This resulting lack of objectivity makes the process very dependent on the mapmaker's skills and experience. Furthermore, the mapmaker will be more inclined to create broad categories of land types to avoid the time-consuming and more error-prone process of making detailed interpretations based on inferred local conditions.

Another approach is based on correlating terrain attributes (ranging from hillslope gradient to bedrock type) of polygons mapped in the field with the incidence and character of landsliding [e.g. Rollerson et al., 1997; Fannin et al., 1997; see Carrara, 1983 and Carrara et al., 1995 for discussion of methodology]. This provides a more quantitative empirical basis for likelihood for failure than is conventionally used in the Washington methodology. Because this is an empirical approach, results can not be extrapolated beyond the area of study. Other recent multivariate approaches based on field measurements, such as that reported by Wiczorek et al. [1997], help identify for particular storm events the spatial controls on hillslope instability. There also exists empirical field-based rating systems, such as the Mapleton "Headwall Rating System" that are not based on quantitative testing but rather intuitive assignment of the relative importance of factors [Swanson and Roach, 1987]. While such intuitive systems may tend to identify unstable areas [Martin, 1997], the lack of a mechanistic foundation makes verification problematic.

A third approach that has been explored in the forest management context is the use of a slope stability theory applied to selected area polygons of similar terrain type or to individual sites on a hillslope. In the Pacific Northwest, the programs DLISA, LISA and 3DLISA developed by Prellwitz [1985], Hammond et al. [1992] and Burroughs et al [1985] [see also Cuthbertson,1992] have been used by the US Forest Service. The infinite slope equation is solved with best estimates (DLISA) or with probabilistic assignment of parameters (LISA and 3DLISA), while some values are back-calculated based on the assumption of a factor of safety at failure [e.g. Kohler, 1998]. DLISA and LISA treat the influence of groundwater as an unknown whereas 3DLISA uses an empirical groundwater response model derived from field observations in the Oregon Coast Range [Burroughs et al., 1985].

While more mechanistic than the empirical approaches previously mentioned, these models appear to be of limited value for several reasons. First, it conceptually inconsistent to divide landscapes into terrain polygons with average properties and then use a mechanistic theory that depends strongly on site-specific conditions. In a threshold phenomenon, such as landsliding, small differences in controls, such as local slope, drainage area or site properties can have a large effect on assignment of stability. Furthermore, these parameter-rich models (these programs require values on soil cohesion, root cohesion, soil bulk density, water table level, friction angle, soil depth, hillslope gradient, and more in the case of 3DLISA) are untestable because the spatial distribution of parameters cannot (with the exception of hillslope gradient) be quantified in any realistic time frame. A probabilistic formulation (in LISA and 3DLISA) has been introduced to try to represent this uncertainty, but this effort while logical is perhaps illusory. Parameters may vary systematically spatially (e.g. thick soils in hollows and thin soils on ridges) and their probability density functions are in many cases probably not independent (e.g. thick soils and ground water characteristics may co-vary). Furthermore, such treatment does not make up for the lack of adequate topographic representation in polygon-based models. The fuller mechanistic understanding of controls on slope stability that is the basis of 3DLISA (and of the model proposed by Sidle, 1992) is nonetheless an important contribution, and is most useful when applied to individual sites that are well quantified, or in exploring, theoretically, possible controls on slope stability.

The fourth approach (which includes SHALSTAB) couples digital representation of the topography, an infinite slope stability model, and a shallow subsurface flow model to predict the spatial distribution of relative slope stability. An early such model is that proposed by Ward et al. [1982]. They used a grid-based model with an assumed static groundwater level and randomly distributed soil depth and root strengths. Okimura and his colleagues

[Okimura and Ichikawa, 1985; Okimura and Nakagawa, 1985; Okimura and Kawatani, 1987; Okimura, 1989; Okimura, 1994] appear to have been the first to incorporate a process-based model for shallow subsurface flow into a digital terrain model for slope instability. They applied the infinite slope model to a grid based representation of landscape topography and estimated the spatial pattern of destabilizing pore pressures using a shallow subsurface runoff model for steady rainfall.

Dietrich et al. [1992, 1993] and Montgomery and Dietrich [1994] took a similar, but simpler approach. Their model was based on the digital terrain model TOPOG [O'Loughlin, 1986] which discretizes the landscape by creating elements bounded by two contour lines and two estimated flow lines (a so-called "contour-based" approach). Unlike Okimura and colleagues they ignored cohesion, thereby avoiding the need to estimate soil depth. They also specifically applied the model in the context of assessing effects of forest management by applying the model to lands being managed for timber in Oregon and California [Montgomery and Dietrich, 1994].

Dietrich et al. [1995] subsequently rederived the fundamental equation used by Dietrich et al. [1992] and included soil depth and a vertically varying saturated conductivity (allowing for systematic differences between the soil and underlying bedrock). Runoff was still treated as steady state. To estimate soil depth (which is necessary in an infinite slope model which includes a cohesion term), they used a process-based soil production and transport model to predict the spatial pattern of soil depth (the foundations of this model were later supported with field studies by Heimsath et al., [1997, 1999]). Furthermore, this model was grid-based rather than contour-based. They found that: 1) significantly less rainfall is necessary for instability if the bedrock conductivity is relatively low compared to the overlying soil than if the bedrock is highly conductive, 2) if the bedrock conductivity is high, instability tends to be focused in unchanneled valleys; 3) ridge soils may tend to be thin and stabilized with modest root strength whereas thick soils in unchanneled valleys require large root strength for stabilization; and 4) root strength change (due to fire, disease, climate change, or land use effects) can have a very large effect on the potential pattern of hillslope instability. Although this model is therefore better able to address issues of forest management because of the incorporation of a root strength term (and a spatially varying soil depth), it also requires much more parametrization than can be practically done over large areas. We will return to this issue later in this chapter.

Three Ph.D. dissertation studies were done in the mid-1990's which explored, among other things, modeling dynamic rainfall-runoff response in predicting the pattern of slope instability [Wu, 1993; Hsu, 1994; and Duan, 1996]. Wu [1993] focused on the issue of timber harvesting strategies (and its subsequent effect on root strength distribution and slope stability). He used a contour-based approach [from Moore et al., 1988] and incorporated a kinematic wave driven groundwater model [see also Wu and Sidle, 1995]. Both Hsu [1994] and Duan [1996] use grid-based models and assumed an exponential decline in saturated conductivity with depth. Hsu used the Dietrich et al. [1995] model for predicting soil depth. As part of a sensitivity analysis both Wu [1993] and Duan [1996] identified soil depth, root strength, and saturated conductivity as important parameters affecting model results. Among other conclusions, all of these studies pointed to the difficulty of parameterization of these controlling factors.

Pack and Tarboton [1997] used the Dietrich et al. [1992] and the Montgomery and Dietrich [1994] model in a grid-based analysis of shallow slope stability patterns in British Columbia and found that the majority of the landslides were strongly concentrated in the least stable ground predicted by the model. Building upon that result they reformulated the model to include root strength (as Montgomery et al. [1998b] have done), added uncertainty estimation of parameters and built an ArcView-based model that they made available on the Internet (SINMAP). We suggest here that such models are very useful, but the lack of spatially registered data on soil and root strength and hydrologic properties make them difficult to parameterize.

SHALSTAB THEORY

Empirical studies of shallow landslides find that they occur on steep slopes and commonly in areas of strong planform convergence (hollows) becausethere soils are thick and shallow subsurface flow is concentrated [e.g. Dietrich and Dunne, 1978; Reneau and Dietrich, 1987; Ellen et al., 1988]. This suggests that surface topography is a primary indicator of where shallow landslides are most likely to occur. For practical application in forest management, it is desirable to construct a mechanistic model that can capture the topographic effects described above. As shown below, we have been able to reduce the model, SHALSTAB, to a point where it can be used with fixed parameters over large areas. The value of such a model is that: 1) it can be applied in diverse environments without costly attempts at parameterization - hence it is fully transportable, unlike empirical correlational approaches; 2) results from different sites can be directly compared; 3) it takes little special training to use the model, and 4) it becomes a hypothesis that is rejectable, i.e. the model can fail - rather than just be tuned until it works. The value of a model that can fail is that it can effectively put a spotlight on processes not in-

cluded in the model that are important. This means the model can help illuminate causality.

SHALSTAB is based on an infinite slope form of the Mohr-Coulomb failure law in which the downslope component of the weight of the soil just at failure, τ, is equal to the strength of resistance caused by cohesion (soil cohesion and/or root strength), C, and by frictional resistance due to the effective normal stress on the failure plane:

$$\tau = C + (\sigma - u)\tan\phi \quad (1)$$

in which σ is the normal stress, u is the pore pressure opposing the normal load and $\tan\phi$ is the angle of internal friction of the soil mass at the failure plane. This model assumes, therefore, that the resistance to movement along the sides and ends of the landslide is not significant.

A further simplification in SHALSTAB is to set the cohesion to zero. This approximation is formally incorrect in most applications. Although the rocky, sandy soils of colluvial mantled landscapes probably have minor soil cohesion, root strength, which can be treated as an additional cohesive term in (1), plays a major role in slope stability [e.g. , Burroughs and Thomas, 1977; Gray and Megahan, 1981; Sidle, 1992]. We have elected to eliminate root strength in this model for the following reasons. First, root strength varies widely, both spatially (over small scales) and in time. Although field studies show that root strength is quantifiable [i.e. Endo and Tsuruta, 1969; Burroughs and Thomas, 1977; Gray and Megahan, 1981], to do so would involve considerable effort. For watershed scale modeling, field-based parameterization of root strength patterns across the landscape would be very time consuming. It is conceivable that remote sensing of canopy types could be used to estimate possible root strength contributions, but such a method, requiring high spatial resolution information has not, to the best of our knowledge, been developed. Secondly, one effect of forest management is to reduce root strength; by assigning a value of zero to cohesion we effectively model the most extreme case- which is a practical boundary to risk assignment. As discussed below, we have somewhat compensated for the absence of root strength by setting the friction angle to a high, but acceptable value.

This is not to say that there is no value in building models with root strength, and several such models exist which employ digital elevation data have been proposed (as discussed above). We now refer to a subsequent version of SHALSTAB in which the soil depth and cohesion are held spatially constant as SHALSTAB.C [used by Montgomery et al., 1998a,b] (and the program is also available at our website). A version of SHALSTAB in which the soil depth varies spatially, the hydraulic conductivity varies vertically and the cohesion is spatially constant is now referred to as SHALSTAB.V [developed by Dietrich, et al., 1995]. We return to a discussion of cohesion later in this paper and show that models that include cohesion, but have no more information than the topographic setting of the landslide, can not be uniquely parameterized (cohesion and friction angle can not be uniquely determined).

By eliminating cohesion, (1) can be written as

$$\rho_s g z \cos\theta \sin\theta = (\rho_s g z \cos\theta^2 - \rho_w g h \cos^2\theta)\tan\phi \quad (2)$$

in which θ is the land surface slope, z is soil depth, h is water level above the failure plane, ρ_s and ρ_w are the soil and water bulk density, respectively, and g is gravitational acceleration (see Figure 2). In this form, we have assumed that there is a relatively small difference in saturated bulk density and bulk density of the moist soil above the saturated zone. This assumption is made to simplify the expression by avoiding the need for another parameter: the bulk density of the unsaturated soil. Derivation of the following equations with this term included suggests that neglecting this effect has a small influence on the results. Subsequently we refer to ρ_s as the wet bulk density, suggesting it represents the integral bulk density of a variably saturated soil. Equation (2) can then be solved for h/z, which is the proportion of the soil column that is saturated at instability:

$$\frac{h}{z} = \frac{\rho_s}{\rho_w}\left(1 - \frac{\tan\theta}{\tan\phi}\right) \quad (3)$$

Equation (3) explicitly states that the soil does not have to be saturated for failure to occur. While saturation is commonly assumed when one analyzes a landslide scar, theoretically it is not necessary. Note that h/z could vary from zero (when the slope is as steep as the friction angle) to ρ_w/ρ_s when the slope is flat ($\tan\theta = 0$). We assume, however, that the failure plane and the shallow subsurface flow is parallel to hillslope, in which case h/z can only be less than or equal to 1.0, and any site requiring h/z greater than 1 is unconditionally stable - no storm can cause it to fail (see Montgomery and Dietrich [1994] for further discussion of terminology of failure potential). Note that $h/z \geq 1.0$ occurs if $\tan\theta \geq \tan\phi(1-(\rho_w/\rho_s))$. We observe in the field that such environments can support saturation overland flow without failing. The value of h/z may locally exceed 1.0 due to exfiltration gradients, such as that observed by Montgomery et al. [1997]. Such processes are not included in the flow model. If the ground slope equals or exceeds the friction angle, then h/z is zero and the site is "unconditionally unstable" or is subject to "chronic"

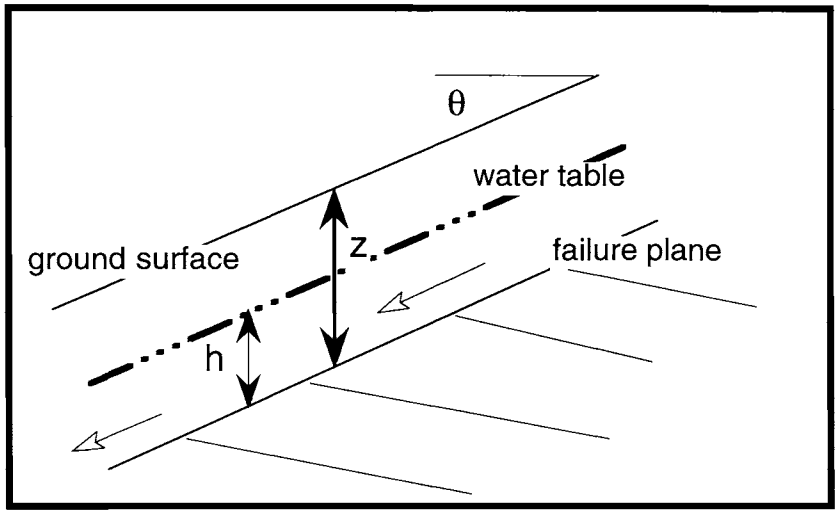

Figure 2. The one-dimensional approximation used in SHALSTAB in which failure plane, water table, and ground surface are assumed parallel. The slope is θ, the height of the water table is h, and the thickness of the colluvium overlying the failure plane is z. Typically the failure plane is at the colluvium-weathered bedrock or saprolite boundary. Open arrows show that flow is assumed parallel to the ground surface.

potential failure; this commonly corresponds to sites of bedrock outcrop.

SHALSTAB links the slope stability model of (3) with a hydrologic model that predicts the topographic controls on h/z. It uses a steady state shallow subsurface flow model to estimate h/z and assumes that the flow is driven by a head gradient equal to the topographic slope. Flow is therefore parallel to the slope (Figure 2). The model actually calculates a water table that is less steep than the ground surface as the h/z increases downslope, but this effect on head gradient on steep slopes is small. Conservation of mass still applies. A key assumption here is that the steady state runoff model effectively mimics what the relative spatial pattern of wetness (h/z) would be during a landslide-producing storm that is not in steady state. If precipitation events are sufficiently intense and of short duration such that thin soils on non-convergent sites can quickly reach destabilizing values of h/z before shallow subsurface flow can converge on unchanneled valleys, then the model will be incorrect. Such a case may have occurred in the 1995 Madison County, Virginia rainstorm, of 770 mm in 16 hours, in which according to Wieczorek et al. [1997] landslides were most common on thin soils mantling planar slopes close to the ridge divide.

In the steady state shallow subsurface flow model, the effective precipitation, q (precipitation minus evapotranspiration and deep drainage), times the drainage area, a, must equal the flow in the conductive soil layer across a cell of width, b, given by Darcy's law, i.e.

$$qa = k_s h \cos\theta \sin\theta b \tag{4}$$

in which $\sin\theta$ is the head gradient, k_S is the saturated conductivity, and $h\cos\theta$ is the saturated thickness measured normal to the ground surface. At saturation the shallow subsurface flow will equal the transmissivity, T (the vertical integral of the saturated conductivity), times the head gradient, $\sin\theta$, and the width of the outflow boundary, b. We can approximate this as follows:

$$Tb \sin\theta = k_s z \cos\theta \sin\theta b \tag{5}$$

Combining (4) and (5) leads to:

$$\frac{h}{z} = \frac{q}{T} \frac{a}{b \sin\theta} \tag{6}$$

Here we see that the pattern of h/z for a given storm is governed by two ratios: one hydrologic ratio and the other topographic. The hydrologic ratio, q/T is the magnitude of the precipitation event, represented by q, relative to the subsurface ability to convey the water downslope for a given head gradient, i.e. the transmissivity. All else being equal, the larger the q relative to T the higher the water

TABLE 1. Conversion values for the hydrologic ratio

T/q (m)	q/T (1/m)	*log (q/T) (1/m)
2512	0.00040	-3.4
1259	0.00079	-3.1
631	0.00158	-2.8
316	0.00316	-2.5
158	0.00633	-2.2
79	0.01266	-1.9

**If the transmissivity is about 65 m^2/day [Montgomery and Dietrich, 1994], a value of log(q/T) of -3.4 means that the steady state rainfall was 26 mm/day, where as a value of -1.9 was 818 mm/day. Each interval of log(q/T) is about a 2 times change in precipitation for a given transmissitivity.

table in the soil, and consequently the greater the number of sites on a hillslope that will become unstable (i.e., the h/z specified by equation (6) exceeds that given by equation (3)). The topographic ratio, a/bsinθ, captures the essential effects of topography on runoff and is composed of two terms: a/b is the topographic convergence that concentrates subsurface flow and elevates the pore pressures, while sinθ is the ground slope for which the steeper the ground, the faster the subsurface flow and consequently the lower the relative wetness defined by h/z. The topographic ratio is nearly identical to that identified by TOPMODEL [Beven and Kirkby, 1979; Beven, 1997] and is very widely used in local and regional hydrologic modeling. The important difference is that TOPMODEL uses tanθ rather than sinθ (as pointed out by Dietrich et al. [1995]). Physically, tanθ is incorrect and while this has no impact on low gradient systems, the error on hillslopes is significant if tanθ is used instead of sinθ. The report by Dietrich and Montgomery [1998] illustrates the behavior of the hydrologic model (and is available at http://socrates.berkeley.edu/~geomorph/).

Setting (6) equal to (3) and solving for the hydrologic ratio gives

$$\frac{q}{T} = \frac{\rho_s}{\rho_w}\left(1 - \frac{\tan\theta}{\tan\phi}\right)\frac{b}{a}\sin\theta \qquad (7a)$$

while solving for the drainage area per outflow boundary length (grid size) for instability gives

$$\frac{a}{b} = \frac{\rho_s}{\rho_w}\left(1 - \frac{\tan\theta}{\tan\phi}\right)\frac{T}{q}\sin\theta \qquad (7b)$$

Equation 7 is the coupled hydrologic-slope stability equation solved by SHALSTAB. The model has three topographic terms that are defined by the numerical surface used in the digital terrain model: drainage area, a, outflow boundary length, b, and hillslope angle, θ. There are potentially four parameters that need to be assigned to apply this model: the soil bulk density, ρ_s the angle of internal friction, ϕ the soil transmissivity, T, and the effective precipitation, q. As we will discuss below, we have found it useful to assign bulk density and friction angle values to be the same everywhere, and compare q/T values, making (7) a fixed-parameter model easily applied across large areas. Of course, if data on soil properties are available, then locally appropriate values could be used.

The ratio of q/T is equal to length per time over length squared per time, i.e. it has the dimensions of 1/length. Throughout this report we will use the metric system, and the unit of q/T will be 1/meters or for T/q it is meters. Likewise, the dimension of a/b is meters. Because q/T is always a small number, we normally use the logarithm of the value in plots (Table 1). The upper and lower bounds of the model are the "unconditionally unstable" or chronic condition and the "unconditionally stable" condition, respectively.

Figure 3 illustrates the relationships between the hydrologic ratio (q/T) and the topographic ratio (broken into a/b and sinθ), for a bulk density ratio of 1.6 and a friction angle of 45 degrees. For a given a/b, the value of log(q/T) at instability for a given slope is shown. In heavy lines are the log(q/T) intervals given in Table 1. The model predicts that hillslopes gentler than 20.6 degrees are unconditionally stable and slopes steeper than 45 degrees are unconditional unstable. Between these two end members, the value of log(q/T) for instability is dominated by the convergence term, a/b, and virtually independent of slope up to hillslope gradients of nearly 35 degrees. Between 30 and 40 degrees the decrease in log(q/T) is only slightly greater than the -0.3 class interval we use in plotting our results on maps. Hence, up to nearly 40 degrees, the SHALSTAB log(q/T) values that would be determined across a landscape are dominated by the convergence term, a/b. Where the landscape becomes very steep (greater than 40 degrees) the gradient term dominates the log(q/T) value for instability.

In order to use SHALSTAB with a digital elevation model, the topographic terms, θ and a/b must be calculated for each grid or element. There is no unique procedure, but there are ones that are less prone to create artifacts. We

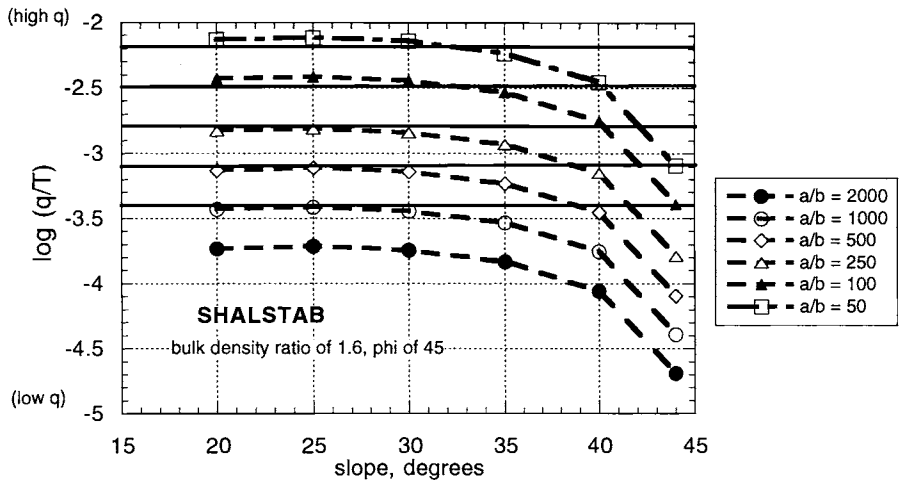

Figure 3. Relationships among log(q/T), surface slope, and a/b for a bulk density ratio of 1.6 and a friction angle of 45 degrees for the model SHALSTAB. The heavy horizontal lines correspond to the log (q/T) values used as boundaries to class intervals used in map production and data analysis.

currently use a grid-based model. Local slope (θ in equation (7)) is estimated as the geometric mean of the slopes in the two cardinal and two diagonal directions across the grid cell, hence all eight surrounding cells are used. This procedure produces results that differ little from the ARC/INFO SLOPE function in the GRID module. Because it uses the eight surrounding cells it will tend to smooth out local variations (associated with just a few cells) in slope, and in some cases will therefore underestimate the local slope. This approach, however, reduces grid artifacts associated with grid noise and with orientation of topography relative to the grid.

We also use a multiple-direction algorithm rather than maximum fall method of distributing area [see discussion in i.e. Quinn et al., 1991; Costa-Cabral and Burges, 1994; and Tarboton, 1997]. The method is similar to that proposed by Quinn et al., in that the proportion of the drainage area each cell distributes to a lower cell, f_i, is equal to the local slope to that cell, S_i, divided by the sum of slopes to all lower cells, i.e. $f_i = S_i/\Sigma S_j$. Extensive testing has shown that this approach gives results that are weakly dependent on the orientation of the topography relative to the grid, as long as cells are not close to the boundaries of the data field (a concern raised by Costa-Cabral and Burges [1994]). As Costa-Cabral and Burges [1994] and Tarboton [1997] point out, this procedure will tend to be "dispersive", i.e. it tends to spread the calculated flow across the slope more than Tarboton's procedure which only permits flow into at most two adjacent cells. Given the diffusive nature of the flow, the broad heterogeneity of the subsurface conductivity field of the subsurface, and the large error in local topography inherent to most digital elevation data, we feel this more dispersive approach which minimizes grid artifact is acceptable.

In SHALSTAB, the proportion of slope in each direction is first calculated. Then starting at a low point in the topography, the contributing line is followed to the divide and then the area to the point at the bottom is calculated. This process is repeated for all cells. The specific catchment area, a/b, in our model is the total drainage area for each cell divided by the cell width.

SHALSTAB VALIDATION

The fundamental premise of SHALSTAB is that sites with the lowest q/T values for instability (least amount of precipitation for instability) should be the least stable and consequently the incidence of shallow landsliding should be highest in these sites. According to SHALSTAB (equation 7), the least stable sites (lowest q/T) have the largest drainage area per unit contour width and steepest slopes. SHALSTAB can be validated once the angle of internal friction and bulk density are fixed, as this leaves only topographic terms on the right hand side of equation (7a).

There are four parameters that could be evaluated in the use of equation (7): $\tan\phi$, ρ_s, T and q. The first three are soil properties and the last is effective steady state precipitation. Each of these parameters also varies spatially, but so far in most applications of SHALSTAB a single value has been assigned to the entire landscape [see Tang and Montgomery, 1995, for an exception]. The three soil properties on average also vary between different landscapes.

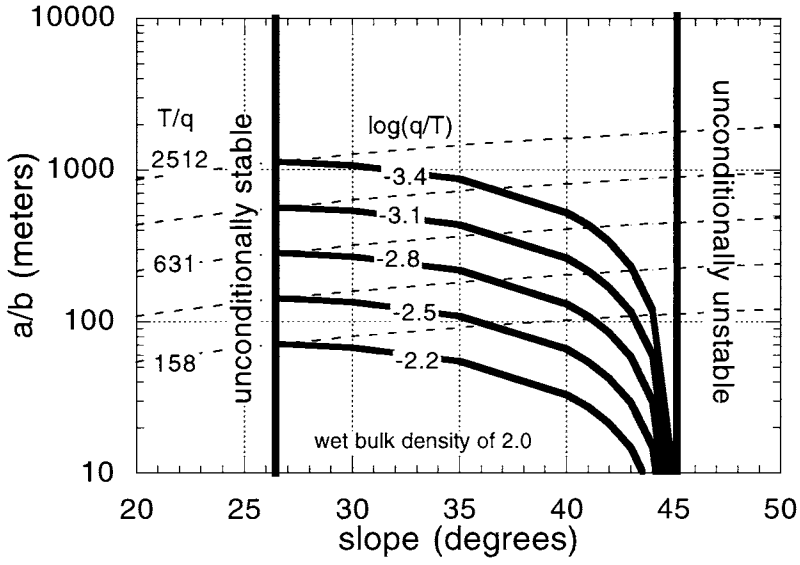

Figure 4. SHALSTAB stability field for bulk density ratio of 2.0 and friction angle of 45 degrees. Vertical heavy lines delineate slopes below which failure will not occur even when the ground is saturated (unconditionally stable) or above which no rainfall is needed for instability to occur (unconditionally unstable). The threshold line above which instability is predicted is shown for a range of log(q/T) values. Note that with increasing q/T the threshold line lowers and a smaller a/b is needed for instability. The dashed lines delineate the threshold of saturation (for each labeled log(q/T) line that intersects it) and is labeled by the corresponding T/q value as expressed in equation (8b). Above the dashed line for the given T/q the land is predicted to be saturated.

In the temperate rainforests of Coastal Oregon, for example, wet soil bulk density is about 1600 kg/m^3 [Torres, et al., 1998] and the friction angle could be as low as the mid 30's [Schroeder and Alto, 1983], whereas in parts of the California coast, the wet bulk density is about 2000 kg/m^3 and the friction angle is in the 40's [Reneau et al., 1984]. Root strength is an important contributor to overall strength, but as mentioned earlier it was eliminated in order to simplify parameterization of the model.

If cohesion is not considered, we have found it useful to set the friction angle equal to 45 degrees, and not let it vary between landscapes. This accomplishes three things: 1) it increases the threshold slope to be more similar to that which would be obtained by a soil with lower friction angle but with some strength contribution from cohesion (see later), 2) by holding it constant, it no longer needs to be parameterized, and the model can be run with only digital elevation data as necessary input, and 3) relative potential hillslope instability can be compared across different landscapes.

The low range of wet soil bulk density that is likely to be encountered in the field has a relatively small effect on the predicted pattern of slope instability when cohesion is neglected. The lower the bulk density, however, the gentler the slope at which instability is predicted to occur. In the absence of field data, it is recommended that a value of 2000 kg/m^3 be used. When comparing results of SHALSTAB run by different groups it is, nonetheless important to note what values of bulk density and angle of internal friction have been used.

Model predictions and field observations on landslide locations can be compared in two ways: comparing field data with model results using graphical representation of equation (7b) or by using equation (7a) to create a map of q/T values. The graphical representation method is described by Dietrich et al. [1992, 1993], and Montgomery and Dietrich [1994]. Note that on a graph of a/b against slope, equation (7b) would appear as a curved line, above which all points would be unstable and below which they would be stable. Figure 4 shows such a plot. The two vertical lines represent the upper and lower bounds to the SHALSTAB model, corresponding to unconditionally unstable or "chronic" and unconditionally stable fields, respectively. The dashed sloping lines which show a/b increasing with slope delineate the threshold for saturation for selected values of T/q, i.e. at saturation

$$qa = Tb\sin\theta \tag{8a}$$

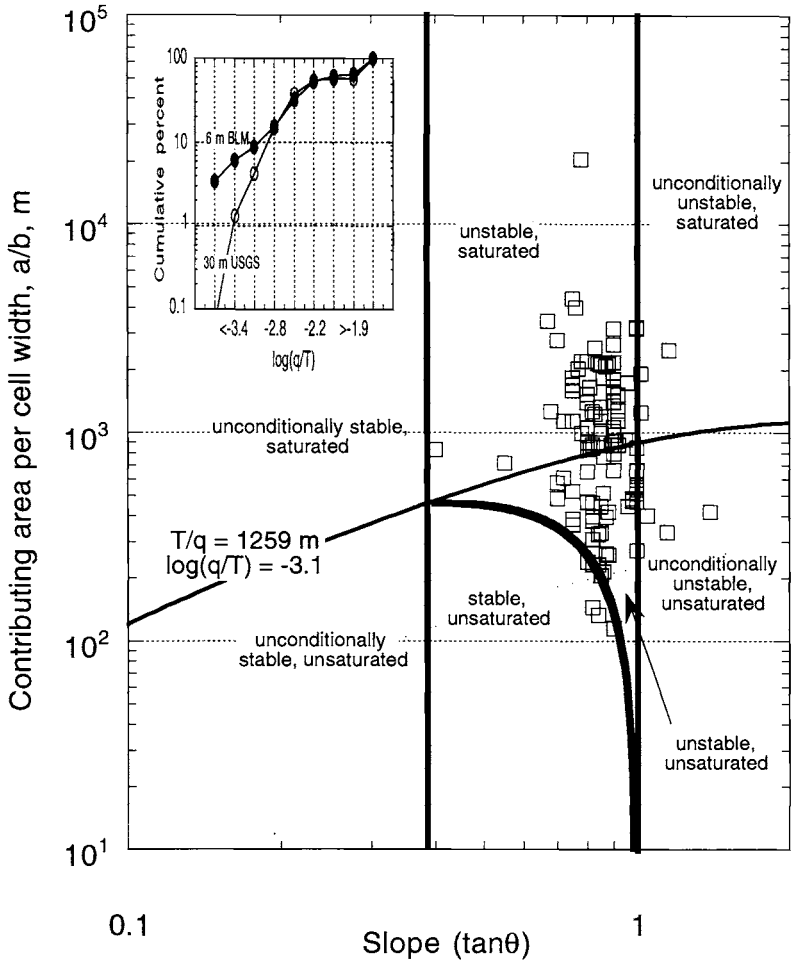

Figure 5. Field observations on a/b and slope for shallow landslides in the Oregon Coast Range plotted against the threshold lines for instability and soil saturation (data collected by the Bureau of Land Management (BLM)). Nearly all data points fall above the threshold curve in one of the four stability fields labeled on the plot. The insert shows the cumulative percent of land area in log(q/T) classes for the study area for 30 m USGS grid data and for data provided from the BLM that could be gridded at 6 m.

which can be written as

$$\frac{a}{b} = \sin\theta \frac{T}{q} \tag{8b}$$

Sites that fall above the dashed lines are predicted to be saturated by the steady state hydrologic model for the corresponding T/q value. The strongly curved solid lines, which terminate at the corresponding saturation lines, define the threshold between stable and unstable topography for selected q/T value, as defined by equation 7b. Each of these lines is labeled with a log(q/T) value which correspond to the T/q values on the corresponding lines of saturation. Figure 4 can easily be used in the field by documenting the drainage area above the scar (a) the width of the scar (b) and the local slope of the slide. If the landslides are concentrated in area of least stability (lowest q/T) then the data should tend to cluster in the upper right hand corner of the plot (above say the -3.1 log(q/T) curve).

Figure 5 shows an example of data obtained from analysis of field data sheets collected by crews working for the Bureau of Land Management in the forested lands of the central Oregon Coast Range. This shows that nearly all of the 93 landslides fall above the curved threshold line for a log(q/T) of -3.1. Each of the seven fields of instability defined by whether the a/b and slope values for a site would cause it to be above or below the thresholds of saturation and slope stability are labeled on the figure. The data are separated by the curve that defines the threshold for satura-

tion (equation 8b). The inset graph shows the cumulative percent of the landscape in successively higher q/T categories for an area of the Oregon Coast range typical of the area where the field data were collected. The 30 m United States Geological Survey (USGS) data are compared with 6 m grid data generated from topographic maps created from aerial photography for the Bureau of Land Management (BLM). The higher resolution topographic map more accurately reproduces the a/b and sinθ than that obtained from field observations, although some fine scale features such as small hollows are still missed by this map. The threshold log(q/T) value of < -3.1 on the 6 m map covers about 9% of the landscape. With a more accurate map, this percent would probably be larger. If one used this field determined threshold value of -3.1 on the 30 m map, the area of potential high instability would be greatly underestimated. If only 30 m data were available, it would be necessary to determine the corresponding log(q/T) value for each landslide site from the digital map and use that to define a threshold log(q/T). We discuss this method below.

Data from aerial photographs can also be plotted on such graphs, but the drainage area and local slope will then be determined from the digital terrain model (or by hand from topographic maps) rather than from field observations. As discussed below, this procedure can introduce relatively large errors because of uncertainty of landslide placement and errors in the digital topography.

An alternative method for model testing is to overlay the location of mapped landslides (either from field or aerial photography) onto a grid map of q/T values. Figure 6a shows an example from the Oregon Coast Range in which landslides were sufficiently small that they were treated as point data and assigned to individual cell locations (The location symbols are much larger than the grid cells). The value of such maps is that one can get a visual impression of model performance, which may have large spatial variation. In this data set, because of survey errors and inaccuracies in the topographic map (see below), there were significant location uncertainties in some of the data points. Figure 6a shows the best estimate of location of the slides. To portray the performance of the model, in Figure 6b we have computed the number of landslides counted in each log(q/T) class (given in Table 1) divided by total area occupied by that log(q/T) class in the study area and plotted that ratio against the corresponding log(q/T) class (using the upper value). If the landslides were randomly distributed with respect to log(q/T) classes the ratio would be the same everywhere (here it would be about 7 slides/km^2). Clearly the landslide occurrence is much more numerous in the log(q/T) classes strongly supporting the model. The two curves in Figure 6b represent the two efforts to locate the slides on the map. In either case, nearly 50% of all mapped landslides fell in log(q/T) values less than -2.8 which represents only 13% of the area of the study.

Two important issues emerge in validation studies. First, the performance of the model is strongly influenced by the quality of the topographic data. Figure 7 shows a shaded relief view of a study site near Coos Bay, Oregon [e.g. Montgomery et al., 1997; Anderson et al., 1997, 1998; Torres et al., 1998] for four different grid scales: 30 m USGS data, 10 m USGS data (obtained from digitized 7.5' quadrangles), 10 m data generated from aerial photography for the Oregon Department of Forestry, and 2 m data generated from an airborne laser altimetry survey [see also Roering et al. 1999; Montgomery et al., 2000]. This illustrates just how crude even 10 m data are compared to the actual topography (which the laser altimetry approximates: note that the roads along the ridge can be seen in this map). Most noticeable is the loss of the fine scale ridge and valley topography (which strongly dictates shallow landslide location at this site) with scale coarsening. This is perhaps best illustrated in Figure 8 where the contour lines of the 7.5' quadrangle and that of the data obtained from the airborne laser altimetry are shown at the same scale. Note the much greater planform curvature in the high-resolution topography (hence greater a/b) and the greater number of valleys. Airborne laser altimetry is just becoming commercially available and techniques for aerial surveying and data analysis are still being developed in forested landscapes. Nonetheless, as figure 7 and 8 clearly illustrate, the technology has arrived and should be exploited for improved landslide mapping.

Figure 9 shows the field of log(q/T) for the four cases shown in Figure 7 on a topographic map where the mapped channel network and landslide scars are shown. This illustrates how the pattern of potential slope instability is strongly affected by the resolution of the topographic data. Note that in the 30 m data, many of the landslides do not occur in the least stable log(q/T) class of < -2.8 (because the convergent areas are not correctly defined), whereas in the laser altimetry data, all the slides fall in the least stable class. The inaccuracy of available topographic maps degrades validation studies, hazard rating assignment, and field studies. All digital terrain based landslide models will suffer from these limitations.

The second issue that arises in validation studies is the problem that landslide size is often larger than a single grid cell, or at least may be mapped as lying in more than one grid cell. This then raises the question of what is the appropriate q/T value for the instability. One could argue, for example, that the average log(q/T) of all the cells lying under a landslide scar polygon should be used. We have used as standard practice that the lowest q/T value in contact with the landslide polygon is the q/T that controls in-

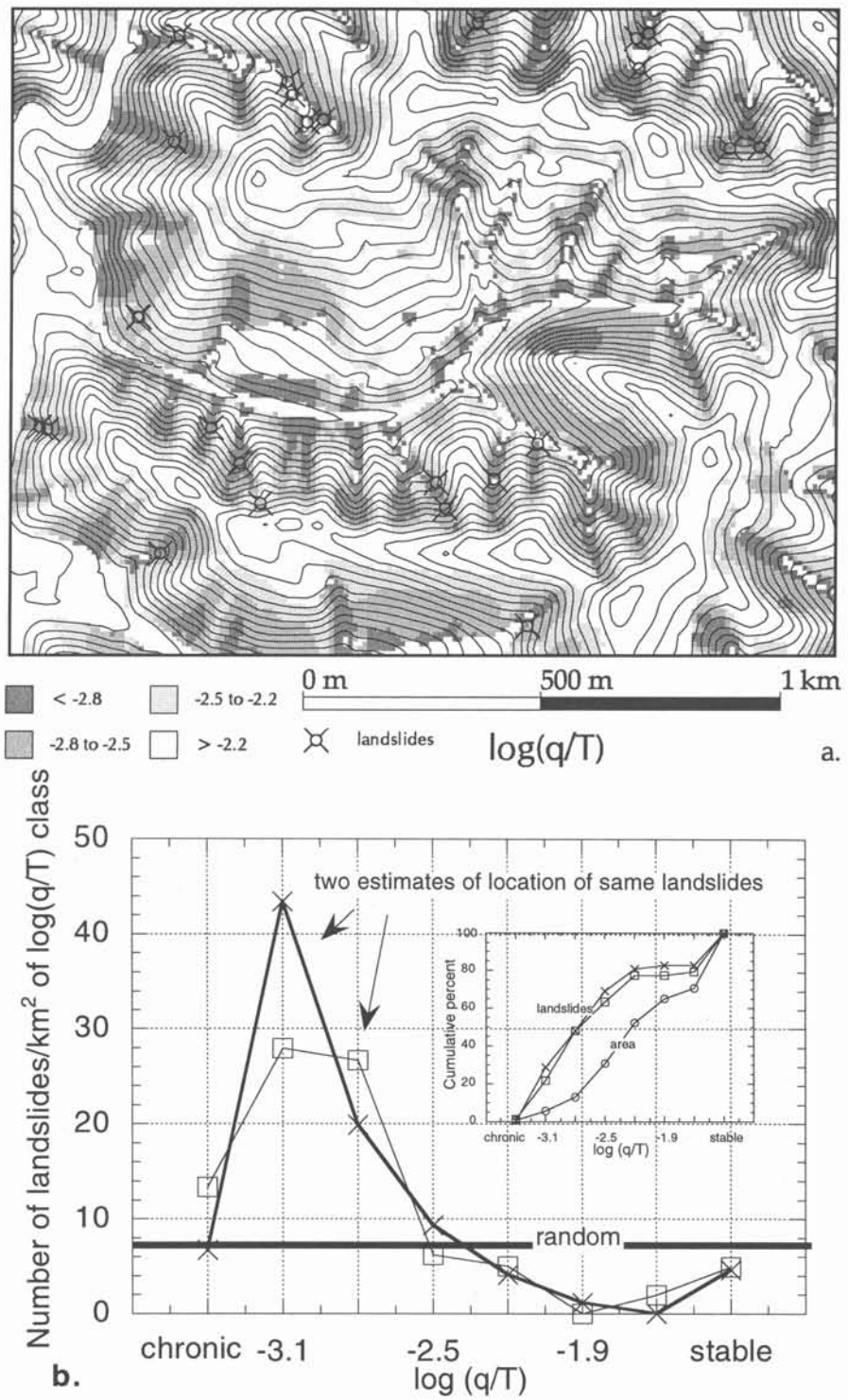

Figure 6. Shallow landslides in the Elk Creek area of the Oregon Coast Range (data provided by the Oregon Department of Forestry). (a) shows the approximate location of the landslides relative to the calculated pattern of log(q/T). (b) shows the landslide density as function of log(q/T). The two curves represent the effect of different estimates regarding the precise location of the landslides mapped in the field. The inset graph shows the cumulative percent of the area in each log(q/T) class (labeled as 'area') and the cumulative percent of number of landslides in each log(q/T) class for each of the two estimates of landslide location. Topographic map is derived from digital data obtained from aerial photographs and then gridded at 10 m.

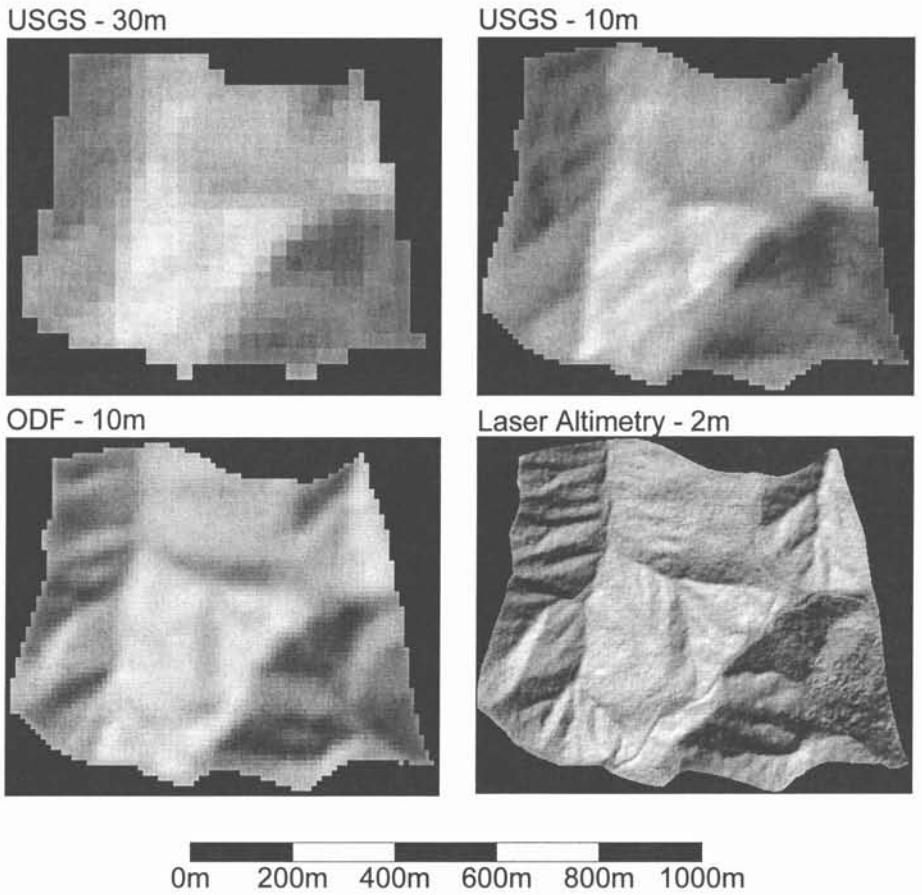

Figure 7. Shaded relief maps of the Coos Bay study area in the Oregon Coast Range based 30 m data from the United States Geological Survey (USGS 30m), digitized contours from the 7.5' USGS quadrangle which was then gridded at 10 m (USGS 10m), 10 m grid data derived from digital data provided by the Oregon Department of Forestry (ODF) derived from aerial photographs (ODF 10m), and 2m girded data obtained from an airborne laser altimetry survey of the site (laser altimetry 2m). Road tread and cuts are visible along the ridge tops on the right side of the laser altimetry image.

stability. There are several reasons for this. Digital elevation generated topographic maps are generally less steep and less convergent than real topography. Hence, the lowest q/T value is perhaps most likely to represent the actual local topography where failure occurs. Including all the other values in a landslide polygon by, say, taking some average, median or some other statistical measure, would tend to systematically include poorly mapped topography, leading to an elevated threshold q/T value and likely lead to a significant overestimation of the extent of potential slope instability. Equally important, most landslide polygons are crudely located. This is because the base maps are inaccurate and because mapmakers commonly don't have the time or resources to carefully locate each landslide on topographic maps. Few mapmakers distinguish between the slide scar (to which the model applies) and the runout track (and this is difficult to do with poor aerial photographs). Scars are commonly mapped as bigger than they actually are- leading to inclusion of topography that is more stable than that associated with failure. Also landslide scars may progressively expand upslope and the landslide mass may run some distance downslope and stop – both of these processes tend to spread the interpreted size of the scar into areas not associated with the initial failure. We propose that picking the lowest q/T value in a polygon may give the most accurate estimate of the local failure condition and avoid problems associated with map resolution and inaccurate mapping of landslide scars.

Our procedure, however, produces a bias toward low q/T. Even randomly located landslides would tend to be

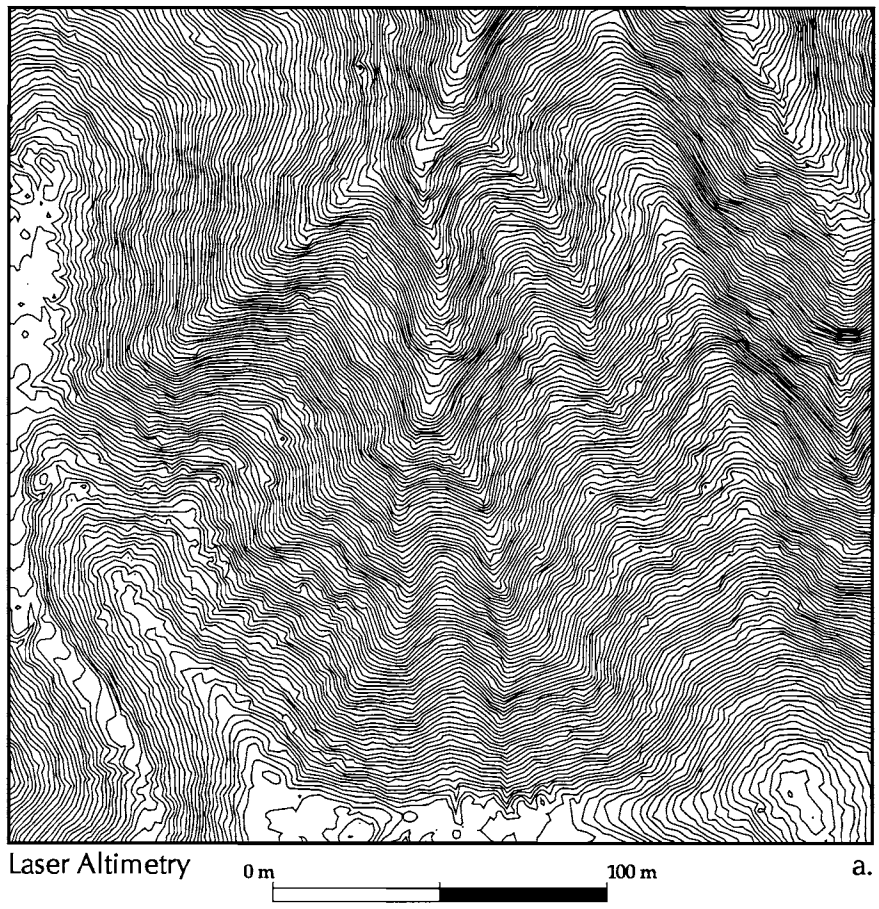

Figure 8. Local comparison of best commonly available data (USGS 10m data) with that obtained from laser altimetry. Contour interval in the USGS data is 12 m while that in the laser altimetry is 1 m.

concentrated in areas having the lowest q/T values because for each randomly located landslide the lowest q/T value would be chosen to represent relative instability category.

Therefore, as a second phase of data analysis, we needed to see if the model would perform significantly better than a similar biased-random model. To answer this question we developed a biased-random landslide generation model to compare with the statistics of the actual mapped landslides. Groups of grid cells of approximately the same size as the median landslide size in a given watershed are randomly placed throughout the watershed until the number of landslides equals the number that had been observed. As is done for the observed landslides, the minimum q/T value within each landslide polygon is selected to represent the value for each landslide generated by the random model, hence we retain this bias. This process is repeated an average of 10 times for each site and the median and standard deviation of the number of landslides found in each log(q/T) category listed in Table 1 are determined. A comparison is then made between observed and randomly generated landslide scars to ensure that any apparent success of the model would not be due solely to bias created by the selection of minimum q/T values. If this bias is large and the model does not perform significantly better than the random model, there would be no observable difference between q/T values for the populations of observed landslides versus the randomly generated landslides. If landslides are preassigned to specific grid cells (often landslides are sufficiently small that they are treated as point data) then a random model would produce a constant landslide density for all log(q/T) classes, as shown in Figure 6b. The random model is a stringent test of the SHALSTAB's results which ensures that we do not draw spurious conclusions about model performance; it is included with our program on our website. We have not attempted to formulate other empirical models against which to test our model performance. While we could find correlations with topography that may perform better than our model, they

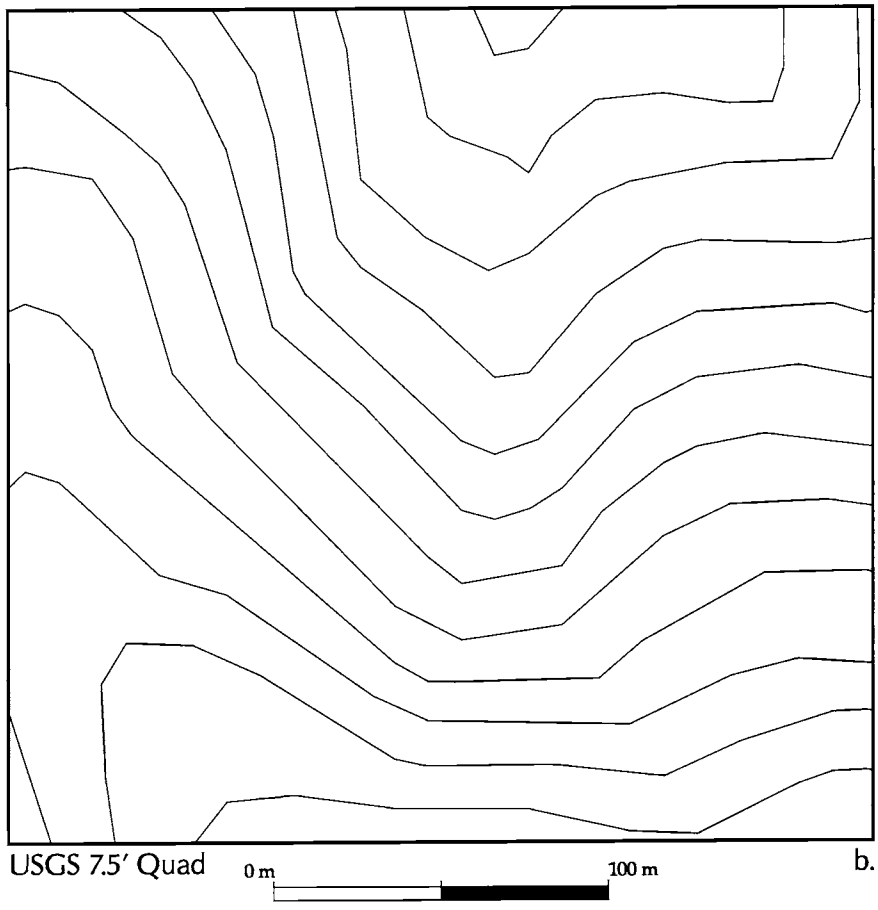

Figure 8 (continued)

would lack the generality of the mechanistic-based approach. Furthermore, the biasing in the random model makes it a difficult model to beat. If model landslides are sufficiently large, then randomly dropped polygons of the same size will have a large probability of intersecting low log(q/T) values. In this case, even if SHALSTAB is accurate, it may not give results significantly different from the biased random model.

The decision to use a single value of log(q/T) to characterize a landslide polygon introduces another concern. The model may be judged as successful because a large percentage of the mapped landslides have minimum log(q/T) values below some low threshold value, such as –2.8, which also differs significantly from the biased-random model. But significant portions of each landslide polygon may overlie higher log(q/T) values. If a hazard map is made using the minimum log(q/T) as a threshold, this map may tend to underestimate the extent of observed landslide area. Hence, by picking the least stable cell to account for a landslide we will tend to underestimate the actual extent of the landslide prone areas [Mark Reid, pers. com., 2000]. This becomes particularly important when using a log(q/T) threshold to delineate high risk areas that may in turn require restrictive land management practices (such as no timber harvest). Without better topographic base maps that show actual topography and permit accurate mapping of landslide location (and avoid the problems with inferior maps described above), we feel that the approach proposed here may be a reasonable compromise between estimating correctly where landslides are likely to occur and not overestimating the extent of high risk area.

Validation Study in Northern California

As part of an assessment of the validity of using SHALSTAB as a tool to guide forest management prescriptions, landslide maps were made from aerial photographs of 7 watersheds in the Northern California Coast Range (Table 2) and compared with q/T predictions using digitized USGS 7.5' quadrangle maps gridded at 10 m [Dietrich et al., 1998]. Aerial photographs taken in 1978 and 1996 of the watersheds, which ranged from 4.8 km^2 to

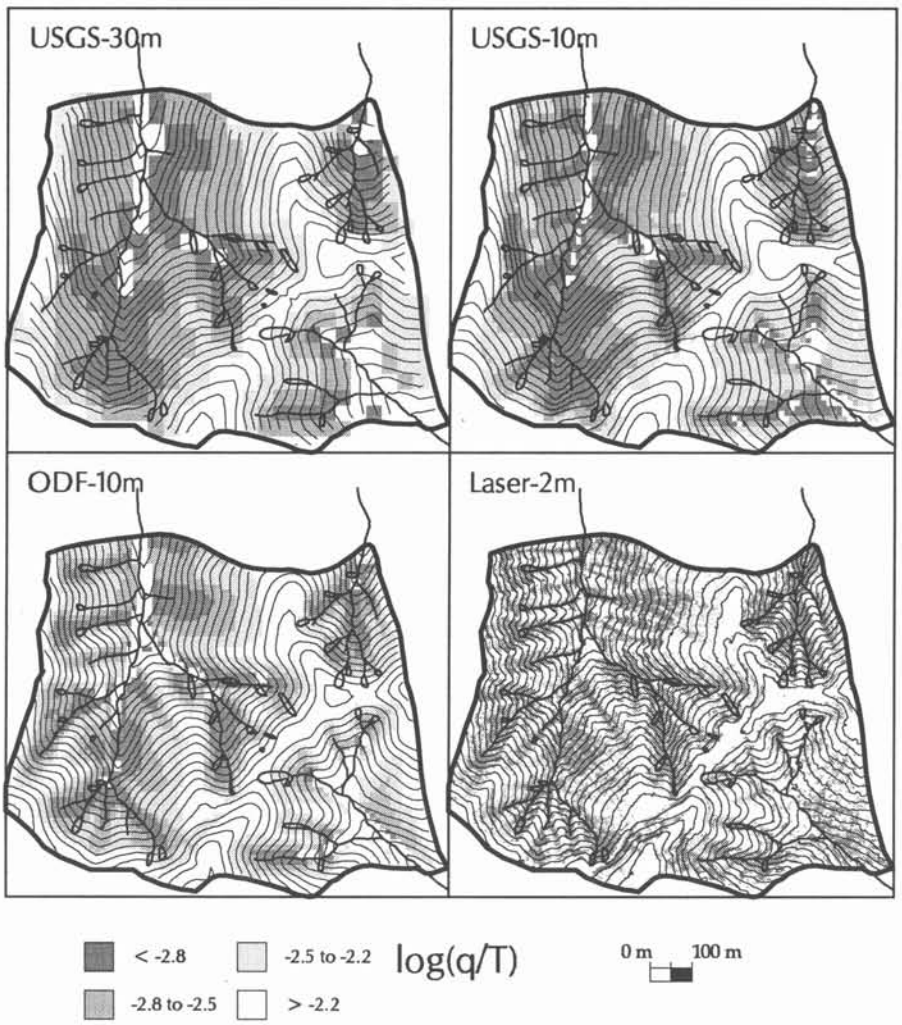

Figure 9. Comparison of SHALSTAB predictions of log(q/T) for the four cases shown in Figure 7 with the location of landslide scars and the channel network (field mapping done by David Montgomery). Contour interval is 5m and bulk density ratio is 1.6.

143 km^2 in drainage area, were used. A total of 844 in-unit failures (i.e. landslides occurring within timber harvest units that were not associated with roads) and 354 road-related failures were mapped in the total study area of 281 km^2. Details of the mapping procedures and all resulting field maps are reported in [Dietrich et al., 1998]. All landslides not associated with roads were classed as in-unit failures because there are no uncut forests in the study sites. Landslides ranged in size from 36 to 17,045 m^2, with a median size of about 500 m^2. Figure 10 shows the results from the largest watershed (the Noyo basin) for the 1996 landslides to illustrate the analysis performed on each watershed. For each site, the number of cells in each log(q/T) category was determined and the resulting cumulative frequency (or percent area) of the total watershed area falling into each successive category is shown in Figure 10a (see curve labeled "area"). This curve shows the predicted potential slope instability across the entire watershed. For the Noyo basin, only about 55 percent of the watershed area is predicted to be unstable. The remaining lands are characterized by gradients too low to fail even when saturated (i.e., classified as "stable"). A classification of "chronic" denotes that the cell is sufficiently steep to be potentially unstable even without the addition of precipitation or runoff (i.e. equivalent to "unconditionally unstable" as defined by Montgomery and Dietrich [1994]). The curve generated by random placement of landslides differs from the total watershed area curve because of the bias that results from selecting only the minimum q/T value in each cluster of cells randomly placed on the landscape. This difference is

TABLE 2: Validation sites in Northern California

WATERSHED	DRAINAGE AREA (Km^2)	NUMBER OF IN UNIT LANDSLIDES	NUMBER OF ROAD RELATED LANDSLIDES	INNER GORGE INCLUDED
Caspar (Spittler) (Field checked)	4.8	29	14	yes
Caspar (Coyle) (1978 &1996)*	21.7	103	none mapped (115 total count)	yes
James (1978 and 1996)	18	72	15 mapped (117 total count)	yes
Noyo (1978)	143	207	42	no
Noyo (1996)	143	222	56	no
Rockport (Juan & Howard) (1978 and 1996)	34	148	214	no
Maple (1978 and 1996)	49.9	43	not counted	no
McDonald (1978 and 1996)	14.6	18	not counted	no

* The dates for each site refer to the date of the aerial photograph used. In each case, the 1978 photographs were black and white and the 1996 were color

large: 26 percent of the total watershed area has an assigned instability value at or smaller than log(q/T) of -2.5, whereas about 51 percent of the randomly placed landslides were assigned log(q/T) values of -2.5 or smaller. The curve for the minimum q/T value for each observed landslide is labeled as "landslides" in Figure 10a and is distinctly different from both the total watershed area curve and the random model curve. The difference largely results from the much greater incidence of observed landslides assigned to the chronic and -3.1 categories. By log(q/T) of -3.1, 58 percent of the observed landslides have been counted, whereas only 21 percent of the random slides and 5.4 percent of the total watershed area has smaller q/T values. This is clear evidence that SHALSTAB has successfully predicted areas with greater probability of failure.

Figure 10b and 10c show landslide density as a function of slope instability category for in-unit and the road-related failures using the Noyo 1996 landslide data. Landslide density is the number of landslides found in a given log(q/T) interval divided by the total area (km^2) included in that category. The density is plotted as a function of the larger bound of that category (e.g., density for the category -3.1 to -2.8 is plotted as a function of -2.8). If the model is not successful at identifying unstable areas (and if there was no bias due to selection of minimum q/T value for each slide), then landslide density should be the same for all instability categories. Because of the bias resulting from using the minimum q/T values, the random landslide density shows a progressively greater concentration of landslides in areas of the highest instability ratings. The curve for observed landslide densities, however, is much different. For log(q/T) values of -2.8 and smaller, the incidence of landsliding was much higher than that estimated from the random placement model. For areas mapped as "chronic" or those falling into the category of log(q/T) < -3.1, the incidence of landsliding is high, equivalent to 9 and 7 landslides per km^2, respectively, for the period recorded by the Noyo 1996 aerial photographs. The large difference in landslide density at low q/T values between the mapped and biased-random placement model demonstrates that SHALSTAB is successful at identifying unstable areas of the landscape and that this finding holds true for both in-unit and road-related shallow landslides. We did not expect the relatively successful performance on road-related landslides because of the large local effects roads have on hydrology, soil strength and topography. This suggests that, at least in our study area, road failures are more likely in steep areas with high a/b – like those found associated with in-unit failures.

Figures 11 through 17 and Table 3 summarize SHALSTAB model performance in this validation study. In each watershed, modeled landslide density was greatest in the most unstable categories and differed substantially from that determined by the random placement model. Figure 11 shows landslide density for observed landslides for each watershed. Landslide density was very high (up to nearly 150 landslides per km^2 of the log(q/T) category) for areas assigned to categories of highest instability. Observed landslide density was greater than that for randomly

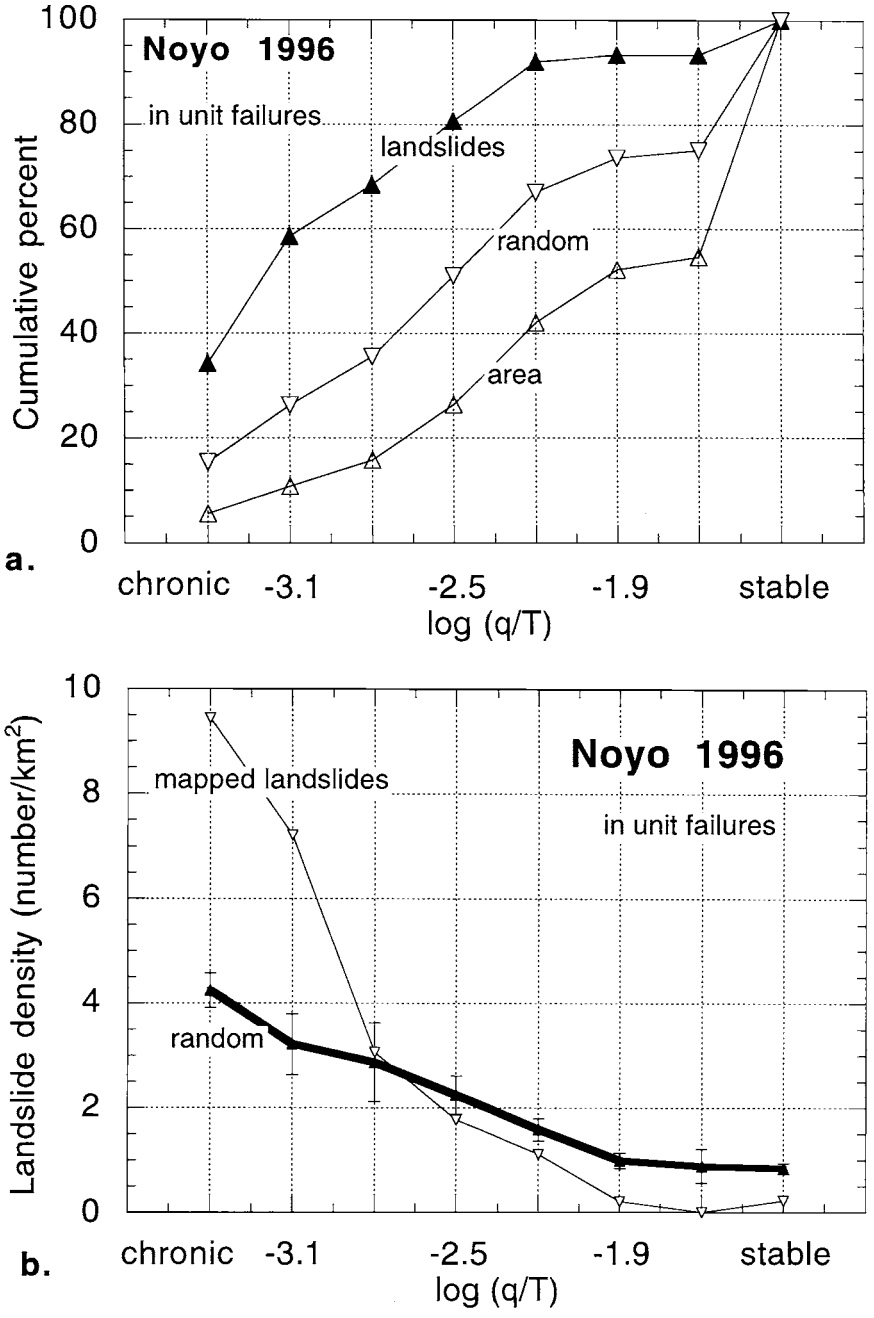

Figure 10. Log (q/T) values for mapped and randomly placed shallow landslides in the Noyo watershed of Northern California. Landslides were mapped from 1996 aerial photographs. Chronic and stable refer to unconditionally unstable and unconditionally stable conditions, respectively. (a) Cumulative percent of watershed area, of random landslides, and of mapped landslides for in unit failures (no influence of roads) as a function of log(q/T) class. (b) Landslide density (i.e. the number of landslides per area of log (q/T) class) for in-unit failures for mapped and randomly placed slides (standard deviation is shown on the random density function). (c) Landslide density for mapped and randomly placed road landslides.

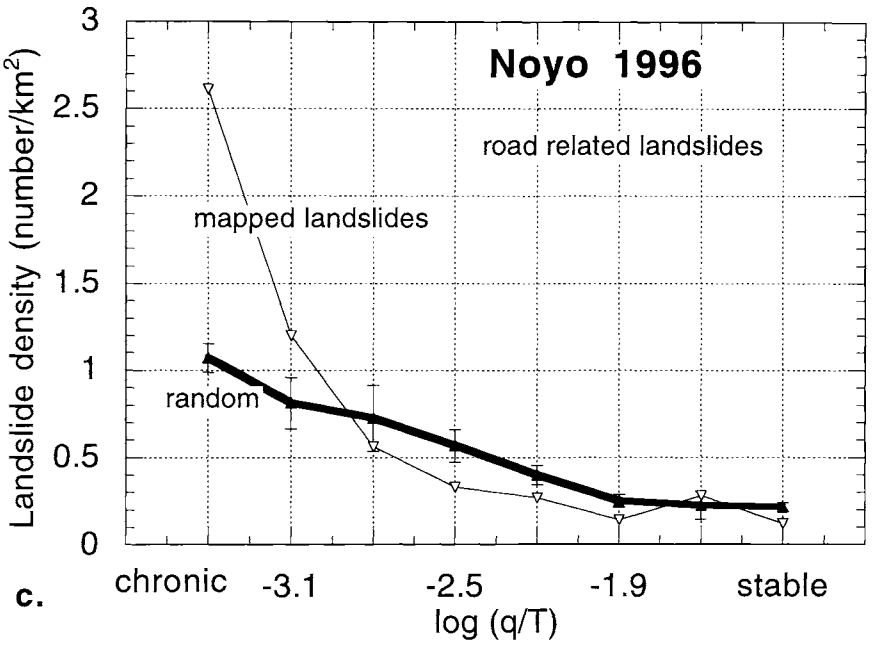

Figure 10 (continued)

placed landslides for log(q/T) values less than or equal to -2.5 for Caspar (Coyle and Spittler). Observed landslide density was also greater than random for values less than or equal to -3.1 for Noyo (1978 and 1996), McDonald (1978 and 1996 combined), Rockport (1978 and 1996 combined) and James. In the Maple watershed, only the landslide density in areas within the chronic category differed from random; however, 26 percent of all landslides occurred in lands of this category.

Figure 12 shows cumulative percentages of landslides found in each log(q/T) category for in-unit landslides in the watersheds. Rockport had the greatest proportion (85%) of landslides in the lowest log(q/T) category whereas Maple had over 40 percent of the landslides falling in the stable category. The high number of landslides mapped in the stable class in the Maple watershed appears to be partly due to the poor quality of the topographic map (and perhaps also the influence of deep-seated landsliding). For all watersheds, the average cumulative percentage of mapped in-unit landslides for the chronic, -3.1, -2.8, and -2.5 categories is 23, 46, 58, and 73 percent, respectively (with a standard deviation of about 19 percent for each category). These numbers are similar for road-related landslides.

Figure 13 shows the cumulative percentage of total area in each landslide instability category for each watershed and the corresponding landslide density based on 1978 aerial photographs. This suggests that the potential for shallow landslide instability is greatest in the Rockport watershed and least in the Maple watershed. In the 1978 aerial photograph coverage landslide density did vary in a manner consistent with watershed potential with Rockport landslide density equal to 4.2 landslides per km^2 and in Maple landslide density of only 0.3. This pattern differed greatly in the 1996 photographs, however, because very little management activity had occurred in the Rockport area since the 1970's and no landslides were detected. Hence, SHALSTAB maybe used as a tool for regional or landscape-scale classification of watersheds for potential landslide hazard, but site specific conditions which dictate when landslides occurs will depend on the management and storm history.

Figure 14 summarizes the validation results and illustrates one measure of risk, by showing the relationship between log(q/T) threshold and watershed area affected. For each instability category, the cumulative percentage of landslides found in that category and cumulative percentage of watershed area were calculated. These two attributes were then plotted against each other to reveal how much of the watershed area would have to be categorized as unstable in order to account for a certain percentage of the mapped landslides. For example, to account for 40 percent of all mapped landslides, about 3 to 8 percent of the total watershed area would have to be categorized as unstable. For 60 percent of the landslides to be accounted for, about 7 to 20 percent of the watershed would be have to be cate-

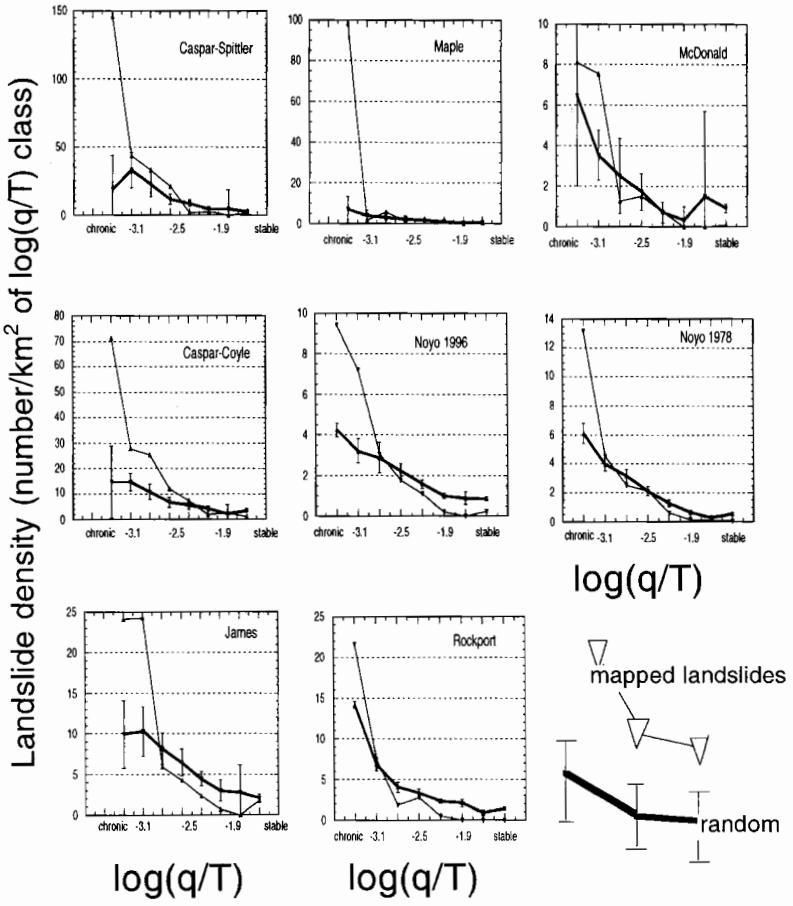

Figure 11. Mapped and randomly-placed landslide density for all the basins in the Northern California study area. Name in each graph refers to watersheds listed in Table 2. The lower, heavy line with the standard deviation bars is the random density. Note that the vertical axis scale varies considerably between watersheds.

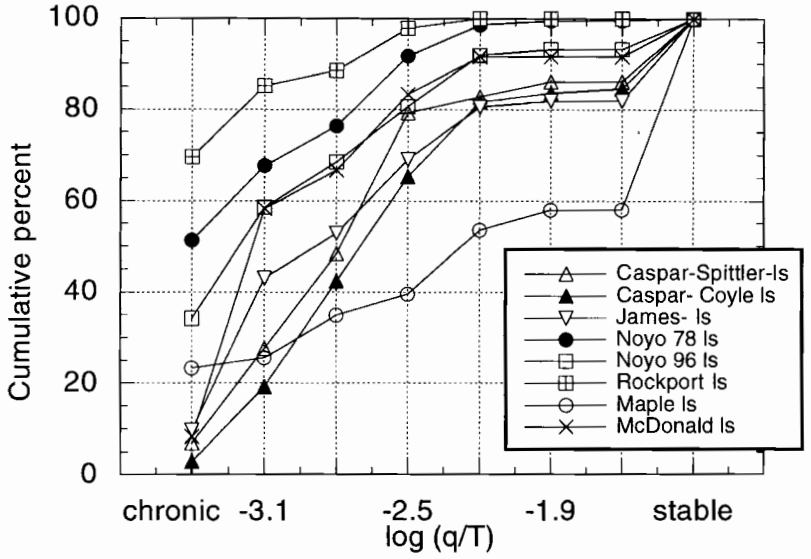

Figure 12. Cumulative percent number of landslides as a function of corresponding log(q/T) for each watershed.

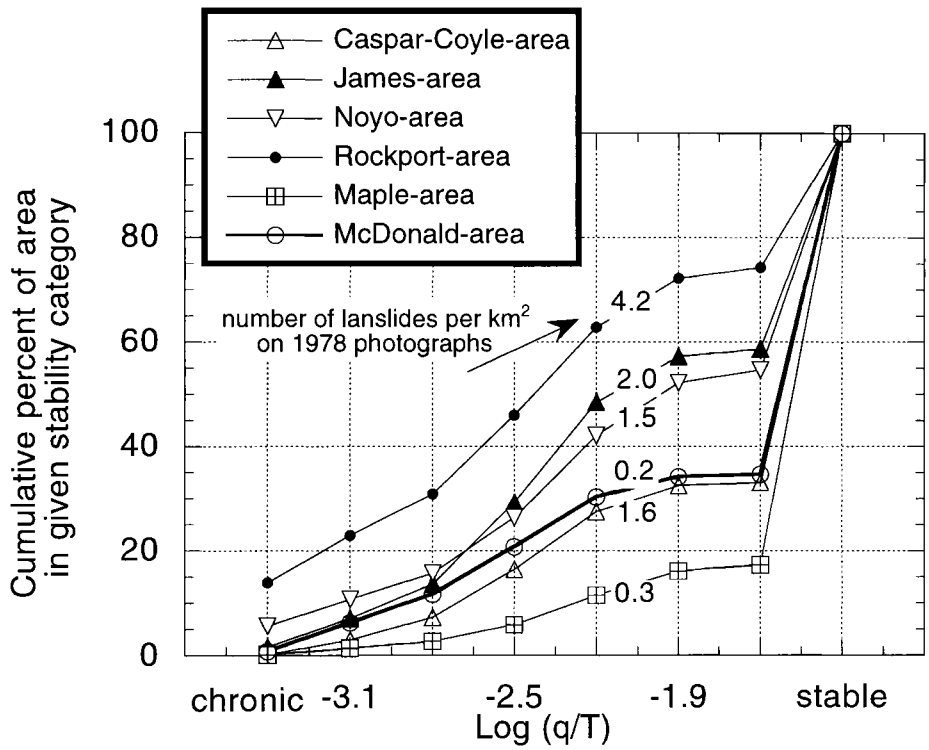

Figure 13. Cumulative percent of the watershed area for a corresponding log(q/T) category and the number of landslides per unit area of the watershed based on 1978 aerial photographs.

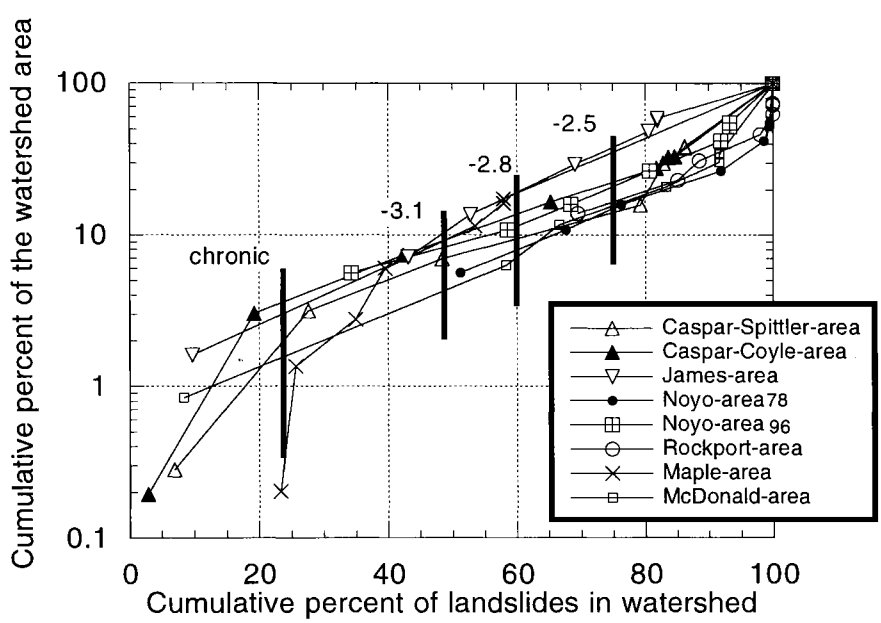

Figure 14. Cumulative percent of the watershed area as a function of the cumulative percent of the number of landslides for progressively larger log(q/T) classes. The vertical lines show the mean cumulative percent of landslides for each log(q/T) class. Each curve starts with the chronic class and each successive symbol along an individual curve records the next larger log(q/T) value (see Table 1 for log(q/T) classes).

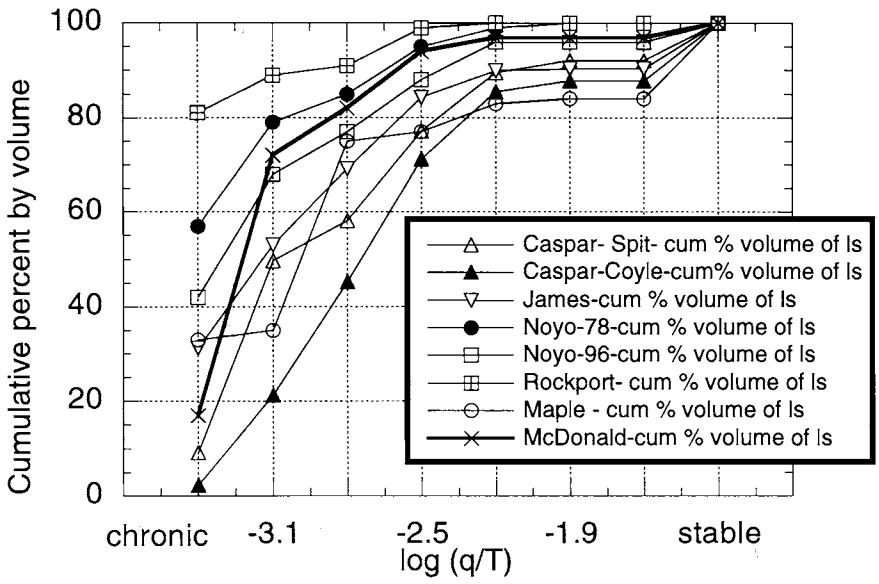

Figure 15. Cumulative percent volume of landslides as a function of corresponding log(q/T) for each watershed.

gorized as unstable. For a given log(q/T) class, however, the range of percent of landslides and corresponding affected area is large. For example, In the Noyo basin about 60% of the landslides fall in the less than -3.1 class, which covers about 11% of the watershed, while in the Rockport watersheds 85% of the landslides fall in the less than -3.1 class, which covers about 23% of the watershed. The average percent of landslides that fall into a given log(q/T) class for the 8 curves is shown as bold vertical lines. An expression fit to all the data shown in Table 3a (ignoring the inner gorge cases) gives $L = 20\ A^{0.43}$ ($R^2 = .87$, n = 21), in which L is the cumulative percentage (by number) of landslides a given cumulative drainage area for any given threshold log(q/T). Hence, this correlation, treating all watersheds as one data set, gives the cumulative number of landslides "hit" as a function of the percentage of the watershed areas classified as high risk. While individual watersheds have different relationships, taken together these data suggest that putting 13% of the area as high risk would include 60% of the landslides, while 20% of the area includes 73%.

The same analysis can be done with the more relevant measure of cumulative landslide volume instead of landslide number. These numbers differ because in four of the watersheds there is a well defined relationship of decreasing landslide size with increasing log(q/T). Such a relationship would be expected if the larger landslides are associated with instability in unchanneled valleys which are typically the least stable elements of the landscape. Landslide area was converted to volume by multiplying the measured plan area by the approximate colluvium depth of 1.0 m (the average of 28 measurements made in the field). Figure 15 shows the cumulative percent of landslide volume and Figure 16 is like Figure 14 except for landslide volume is used instead of landslide number. In general the model performance is improved, i.e. for the < -3.1 class the percent volume is on average 58 percent (as compared to 46 percent by cumulative number), for < -2.8 it is 73 percent (as compared to 58 percent) and for < -2.5 it is 86 percent (as compared to 73 percent). A correlation of cumulativelandslide volume (V) against cumulative watershed area gives $V = 33\ A^{0.3}$ ($R^2 = 0.67$, n = 21). Hence, the plots shown in Figures 14 and 16, and the related correlations can be used to define the tradeoff between maximizing the number of landslides predicted to occur in a high hazard zone and the minimizing the amount of area that must be classified as high hazard.

Table 3 summarizes model performance by log(q/T) class for each watershed by number (Table 3a) and by volume (Table 3b). For comparison among the watersheds, the cumulative percent watershed area for which the corresponding cumulative log(q/T) class accounts for approximately two-thirds of the number or volume of mapped landslides is labeled. This area ranged from as little as 3% to as high as 23% of the total watershed area. In Northern California, slopes immediately adjacent to channels are often quite steep, and noticeably steeper than upslope areas. These inner gorges are rarely accurately portrayed on

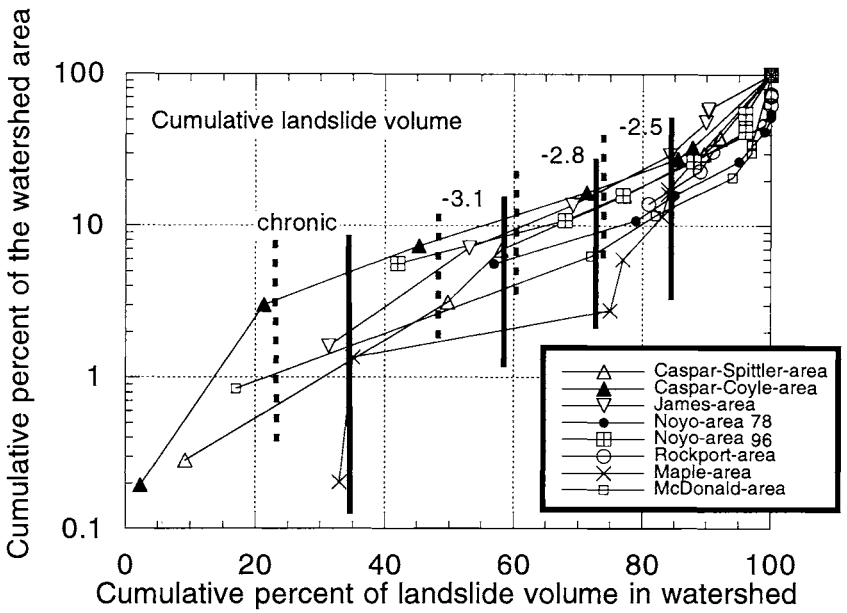

Figure 16. Cumulative percent of the watershed area as a function of the cumulative percent of the volume of landslides for progressively larger log(q/T) classes. Heavy vertical lines record the average cumulative percent volume of landslides for each log(q/T) class; the dashed lines show the same thing for cumulative percent by number (as in Figure 14).

standard 7.5' USGS topographic maps but are common places for shallow landsliding. Hence, further delineation of high-risk areas may be obtained by mapping inner gorges and adding them to the high-risk category. For two of the basins (Caspar and James), the inner gorge was mapped from aerial photographs by the California Division of Mines and Geology (CDMG) and reported in quadrangle-based landslide maps. Although a large percentage of the landslides (35 to 69 percent) fell within inner gorge areas, so did a large percentage of total drainage area (12 to 20 percent). Consequently, a greater percentage of the landslides in each watershed (i.e., Caspar-Spittler, Caspar-Coyle, and James) could be associated with a smaller percentage of the landscape area if SHALSTAB alone (without including the inner gorge) was used without separate delineation or classification of inner gorge areas using the available CDMG maps. This outcome probably depends on the quality of the topographic map and how accurately inner gorge areas are delineated on the CDMG maps. The best solution is to obtain higher resolution topographic maps (from laser altimetry for example) so that the inner gorge is well represented in the topographic base.

The cumulative percent area versus percent landslides for a given log(q/T) for the Northern California study area is similar to that found for similar quality topographic maps in the Oregon Coast Range (Elk Creek-Figure 6a and Coos Bay-Figure 9) (Figure 17). The use of higher quality (laser altimetry) data creates a very different relationship. For the laser altimetry-based analysis, all 36 of the landslides fell in the < -3.1 log(q/T) class.

APPLICATION OF SHALSTAB IN FOREST MANAGEMENT

In all applications a decision must be made as to what constitutes "high", "medium" and "low" hazards, i.e., the log(q/T) class cutoff that delineates the sites of greatest concern. Typically these different classifications will receive different land use limitations. For example, high risk areas may be classified as no timber harvest areas or they may be simply used to flag areas that should be reviewed by geologists. One approach would be to: 1) obtain the best possible topographic base; 2) use field observations and aerial photographs to create a map of landslide scars (noting which slides are due to land use activities) and locate accurately these scars on the topographic data base; 3) use output from SHALSTAB to determine a log(q/T) value for each scar; and 4) use the number of landslides associated with different log(q/T) values and some measure of risk (both environmental and economic) to guide in the decision as to what threshold values to assign. Additionally, to further evaluate model performance it can be

TABLE 3a. Summary of validation results based on number of landslides in each category

Watershed	cumulative percentage (by number) of mapped landslides (in unit) in modeled slope stability category (log q/T)			
	Inner Gorge	-3.1**	-2.8	-2.5
Caspar (Spittler)	69 *(20%)**	76 *(21%)*	86 *(23%)*	97 (30%)
	---	---	---	---
	n.a.	28 *(3%)*	48 *(7%)*	79 *(16%)*#
Caspar (Coyle)	42 *(20%)*	45 *(22%)*	59 *(24%)*	75 *(30%)*
	---	---	---	---
	n.a.	19 *(3%)*	42 *(7%)*	65 *(17%)*#
James	35 *(12%)*	63 *(17%)*#	68 *(23%)*	79 *(36%)*
	---	---	---	---
	n.a.	43 *(7%)*	53 *(14%)*	69 *(29%)*
Noyo (1978)	n.a.	68 *(11%)*#	76 *(16%)*	92 *(26%)*
Noyo (1996)	n.a.	59 *(11%)*	68 *(16%)*#	81 *(26%)*
Rockport	n.a.	85 *(23%)*#	89 *(31%)*	98 (46%)
Maple	n.a.	26 *(1%)*	35 *(3%)*	40*(6%)*
McDonald	n.a.	58 *(6%)*	67 *(12%)*#	83 *(21%)*

TABLE 3b. Summary of model results (for volume)

Watershed	cumulative percentage of volume of mapped landslides (in unit) in modeled slope stability category (log q/T)		
	-3.1**	-2.8	-2.5
Caspar (Spittler)	50 *(3%)**	58 *(7%)*#	77*(16%)*
Caspar (Coyle)	21 *(3%)*	45 *(7%)*	71 *(17%)*#
James	53 *(7%)*	69 *(14%)*#	84 *(29%)*
Noyo 1978	79 *(11%)*#	85 *(16%)*	96 *(26%)*
Noyo 1996	68 *(11%)*#	77 *(16%)*	88 *(26%)*
Rockport	89 *(23%)*#	91 *(31%)*	99 (46%)
Maple	35 *(1%)*	75 *(3%)*#	77*(6%)*
McDonald	72 *(6%)*#	82 *(12%)*	94 *(21%)*

*percentages (in itallics) refer to cumulative percent of area in this slope stability category
**cumulative percent includes the chronic category
#log(q/T) category which accounts for about two-thirds of the landslides

useful to compare the results from mapped scars with those produced by other means, such as the biased-random model proposed here, or to compare the performance of SHALSTAB with other models. Both maps and plots (showing where the landslides occur on the a/b versus slope graph (i.e. Figure 5)) are useful. This analysis can be done in a fixed parameter mode, or optimization can be attempted by allowing parameters to vary (producing location specific results).

Experience with SHALSTAB [Montgomery and Dietrich, 1994; Dietrich et al., 1998a,b] suggests that a threshold value for which a large proportion (about 60% to 80%) of shallow landslide scars occur depends on the quality of the base map, but in general, a value of log(q/T) -2.5 will capture the vast majority of the scars (up to 100%). In the three small test sites reported by Montgomery and Dietrich [1994] between 83 and 100% of all scars fell below the -2.5 threshold (using 5 m contour interval data). A study in the upper Chehalis watershed in Washington in which 629 landslides were mapped (including 470 that were road-related) found 86% of all the scars in values below a log(q/T) of -2.5 using 30 m grid data [K. Sullivan, pers. com., 1994]. A modified version of SHALSTAB (using a spatially constant cohesion and soil depth) was applied to 3224 landslides in 14 watersheds in Oregon and Washington and about 66 percent of the landslides occurred in less than the log(q/T) of -2.5 using mostly 30 m grid data [Montgomery et al., 1998b]. Montgomery et al., [2000] also show that the cohesion based SHALSTAB.C was better than the biased-random model below log(q/T) values of –2.2. In the Oakland hills, just south of the University of California, 84% of the 78 scars were found below log(q/T) of -2.5 using 10 m grids (unpublished data). In the Northern California validation study described above 71 to 99% of landslide volume occurred in cells with log(q/T) less than -2.5 using 10 m grid data.

For forest management decisions, the general goal would be to reduce shallow landsliding to an appropriate level by restricting management on as small a fraction of the landscape as possible. Based on our analysis in the Pacific Northwest, in order to capture more than two-thirds of the landslides, for 30 m grid data, a threshold of -2.5 appears to be needed, for 10 m data (from digitized 7.5' quadrangles) a threshold of -2.8 may be adequate, and for still higher resolution data this threshold may be pushed to -3.1. Comparison with the biased-random model indicates

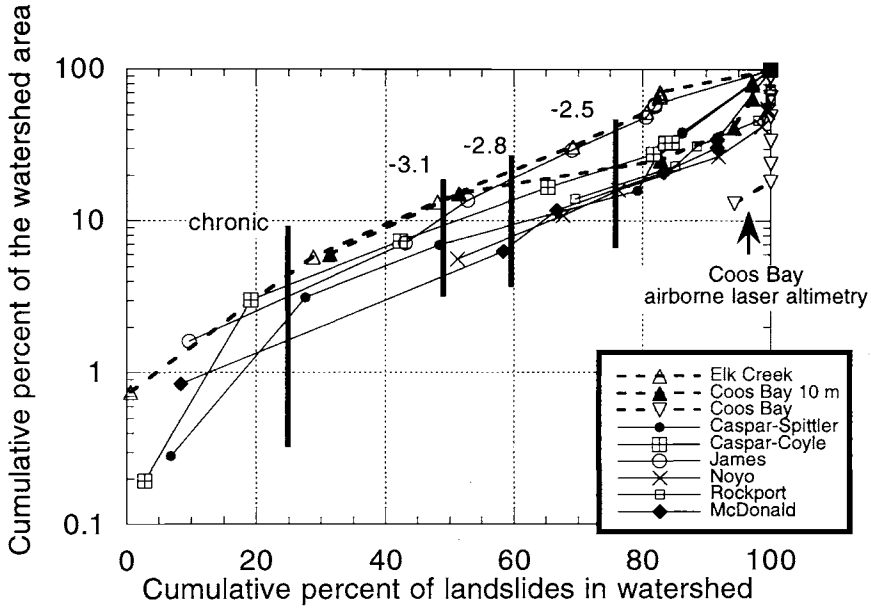

Figure 17. Cumulative percent of the watershed area as a function of the cumulative percent of the number of landslides for progressively larger log(q/T) classes for Northern California and Oregon Coast Range watersheds. The Coos Bay 10m data are for the USGS 10 m data shown in Figure 9, where as the data labeled 'Coos Bay' are derived from the laser altimetry, also shown in Figure 9. Elk Creek refers to the data shown in Figure 6.

that for the 10 m case and with relatively large mapped landslides, SHALSTAB can't distinguish observed from randomly placed sites for a log(q/T) > -2.8. Lacking additional data, we recommend the above threshold values of log(q/T). Specific site studies may find otherwise. For example, Pack and Tarboton [1997] using their own computer code based on SHALSTAB accounted for 91% of their mapped landslides using a threshold log(q/T) of -3.3 for a 20 m grid of the 730 km^2 Trout Lake Basin in British Columbia.

Ultimately, the choice of the high hazard cutoff and consequent land use prescription will implicitly or explicitly reflect the user's perspective on risk. The higher the threshold, the greater the likelihood that all shallow landslides will be accounted for, but also the greater the watershed area that is classed as high hazard. Perception of risk will probably differ depending on the value of the resource that shallow landsliding may threatened (e.g. endangered fish, roads, or houses).

Three kinds of applications of SHALSTAB to forest management issues have been explored or considered. One application has been its use by public agencies (e.g. Bureau of Land Management) or by private companies in watershed analyses that lead to site-specific prescriptive measures. For example, Mendocino Redwood Company (MRC), which was created from lands purchased from Louisiana-Pacific in Northern California, is using maps produced from SHALSTAB in a variety of ways. The maps have been combined with a channel rating system to delineate watersheds that have the greatest potential for high value aquatic resources and high potential shallow landsliding (either from in-unit failures or road failures). These watersheds are considered most at risk and are to be given priority for watershed analysis [Olsen and Orr, 1999]. The maps have been used as part of MRC's watershed analysis process. SHALSTAB maps in combination with aerial photograph analysis and field mapping are used to develop mass wasting map units which are assigned watershed specific land management prescriptions [Chris Surfleet, pers. com., 2000]. SHALSTAB is also used as a tool, along with other information to determine risk of instability and assign local prescriptions. Specifically the MRC policy is: "no harvest activity will occur, with the exception of cable or helicopter harvesting that retains over 50% of the pre-harvest basal area, or any construction of roads and landings in areas defined in the field as having a significant likelihood of sediment delivery from mass wasting unless a site-specific assessment is conducted and operations approved by a registered geologist" [Chris Surfleet, pers. com., 2000].

Another application is in regional planning analyses performed by government agencies. For example, we have

Table 4. Cumulative percent of landscape in each landslide hazard category

log(q/T)	***Allegany	Golden Falls	Greenleaf	Mapleton	Heceta Head	Cedar Butte
*chronic	<1	<1	<1	<1	<1	1
<-3.4	1	2	1	1	2	7
-3.4 to-3.1	3	5	4	4	6	14
-3.1 to -2.8	11	13	15	14	17	29
-2.8 to -2.5	30	28	38	33	35	53
-2.5 to -2.2	49	40	55	47	47	71
-2.2 to -1.9	54	42	58	49	49	77
> -1.9	54	42	58	49	49	77
**stable	100	100	100	100	100	100

* chronic = slope equal to or greater than 45 degrees
**stable = slope less than 20.6 degrees
*** 7.5' quadrangle in Oregon Coast Range (30 m data)

run SHALSTAB on the entire Oregon Coast Range using 30m USGS data to provide basic data on relative potential slope instability to the National Marine Fisheries Service. This was done to help inform the debate about regional plans for protecting and restoring coho salmon in the Oregon Coast Range. Table 4 shows examples of results from selected quadrangles, showing that in the southern highly dissected part of the range, the proportion of area in each log(q/T) class is similar, whereas in the very steep topography in the northern part of the range, a much greater proportion of the area is in the low log(q/T) classes. If the log(q/T) threshold for high hazard were -2.5, then, in the highly dissected portions of the range, upwards of 30% of the landscape would require field review by a specialist because it would be classed as high hazard. This value is halved if the threshold is lowered to -2.8. These tables and accompanying maps provide a useful quantitative assessment for regional planning purposes.

A third application is in hazard mapping with regard to structures and people. With increasing development in areas adjacent to lands managed for timber production, the risk that forest practices will lead to destruction of houses and loss of life is increasing. SHALSTAB only maps the spatial pattern of relative potential for shallow landslides: it does not delineate debris flow runout path or distance. The simplest approach to include the runout is to define a threshold channel slope below which debris flows typically stop and then map separately all channels above and below this threshold [i.e. Montgomery and Dietrich, 1994; Dietrich and Sitar, 1997]. Other procedures exist, most notably that of Benda and Dunne [1997] which includes the effects of tributary junction angle on runout distance. Steep valleys fed from drainage areas with areas of low q/T present the greatest risk. In order to include debris flows that run down unchanneled valleys, the threshold for channel initiation used in a digital terrain prediction of the channel network needs to be set fairly low.

Ideally, the forest practices decision (or prescription) for a site that is rated as high potential for instability could be conditioned by the risk downslope. If structures or people are at risk, then clearly the most stringent restrictions should apply. Presumably high restrictions would apply for river systems in which aquatic resources have been greatly diminished. If the sediment that could be released from a shallow landslide cannot be delivered to the river system (for example if the sediment were to be deposited on a debris fan on a terrace that does not drain via a channel to the river system) there is reduced value in restricting forest practices at the potentially unstable site. If sediment arrives in a steep, non fish-bearing stream that is connected to the river network, however, that sediment has been "delivered" and should not be discounted, as it still can contribute to sediment loading downstream.

Presently, there seems to be little knowledge about what might be an acceptable frequency of timber harvest related increase in landsliding and resultant river sedimentation to a river ecosystem. In fact, some have argued that debris flows can be beneficial to aquatic habitat [Reeves et al., 1995]. While the concept that debris flow delivery of coarse sediment and wood to sediment deficient and wood free streams can create important aquatic habitat is useful, its practical application requires considerable knowledge of the river system. Specifically one might argue that it is desirable to cut and destabilize an area because of the perceived need for coarse sediment downstream (in, say, bedrock dominated channels). There are several problems with this idea. The notion that further disturbance of potential failure sites is beneficial ignores the fact that there are no extensive areas under industrial forestry in the Pacific Northwest that have not already experienced some level of timber harvesting or land use related fires, and consequently are in a reduced state of stability. It would take extensive, detailed field studies of all potential sites to demonstrate that without further timber harvesting the rate of debris flow generation would be too low. Cutting and removal of wood from potential landslide source areas also eliminates what might be a primary source of large woody debris replenishment. Furthermore, most river systems

have been altered through some combination of such things as large woody debris removal, splash damming, gravel mining, stream side timber harvesting, and dams such that considerable care must be taken to infer simple causal relationships between debris flows and channel habitat.

DISCUSSION

The model SHALSTAB is an attempt to create a simple mechanistic model that can be widely used to delineate relative potential for shallow landsliding in the absence of spatially registered soil strength and hydrologic properties. Because of its simplicity, it can be validated with field studies. At present we know of no application in which the model demonstrably failed, but we can think of cases in which it should. In areas in which shallow landsliding is associated with the active toes of large-deep seated landsliding the model may fail because of the low gradients and strong lithologic control on location of deep-seated landsliding. The mechanisms of mass wasting are different in deep-seated slides. If short, intense rains dominate shallow landsliding, then convergence effects of surface topography on shallow subsurface flow may not operate, and, consequently, the shallow landsliding may not depend strongly on a/b (as is suggested by Wieczorek et al.[1997] for a storm in Virginia). There are circumstances in which the topography is favorable for the generation of shallow landsliding, but the incidence is very rare due to lack of soil mantle, high soil strength, or insufficient rainfall. One such area is the glaciated, bedrock-dominated landscape of the Sierra and Cascade Mountains.

Several points need to be stressed about the interpretation and limits of SHALSTAB. Even if all mapped shallow landslides in a region occur in the lowest log(q/T) classes, the vast majority of the low log(q/T) sites in the study area will show no evidence of shallow landsliding. The things that have been eliminated from the slope stability model dictate the timing and size of failure at individual sites. Spatial and temporal variability in such properties as soil cohesion, root strength, soil depth, hydraulic conductivity fields of the soil mantle and underlying bedrock, antecedent moisture and storm history, and land use alterations of hydrology (e.g. changes in evaportranspiration, diversion of road runoff to unstable sites) are unknowable at all potential sites across a landscape, making the prediction of the exact time and location of shallow landsliding impossible. Hence, the SHALSTAB map is solely a portrayal of the effect that surface topography has on the relative potential for instability. All these other factors bear on whether the site actually fails in some interval of time. If most shallow landslides occur in low log(q/T) areas, then the SHALSTAB map is simply showing those places on the landscape that are topographically similar to those that failed, and therefore, without further information about individual sites, should be considered equally likely to fail.

It is often thought that the effective precipitation term, q, in the model can be interpreted in terms of precipitation characteristics in an area, i.e. the rainfall amount can be related to a particular storm frequency and magnitude. The hydrologic model in SHALSTAB is based on steady state precipitation and runoff, hence q specifically would be a precipitation event of sufficient duration that steady state runoff is obtained, a condition rarely if ever experienced under natural storms. Nonetheless, it can be useful to estimate an average transmissivity (T) and compare the calculated precipitation (q) for a given log(q/T) category to rainfall characteristics in an area. For example, based on detailed fieldwork at an experimental site in coastal Oregon [e.g. Montgomery et al., 1997; Anderson et al., 1997, 1998; Torres et al., 1998], Montgomery and Dietrich [1994] estimated the transmissivity to be about 65 m^2/day. This gives an effective q of 0.05 m/d for a log(q/T) of -3.1, a reasonable multi-day precipitation rate, but gives a value of 0.2 m/d for a log(q/T) of -2.5, which simply does not occur over the several day period that would be needed to reach equilibrium. With sufficiently detailed topographic data (such as shown in Figure 7), this kind of calculation may place some limit on reasonable values of log(q/T) for instability to occur.

SHALSTAB does not predict either the size of individual scars nor the rate of landsliding. The model is based on the infinite slope approximation, and therefore, it can not specify a specific size, other than the artificial size of the grid chosen for the analysis. Okimura [1994] discusses a method using a three-dimensional analysis in a digital terrain model to estimate size. Furthermore, the rate of landsliding remains problematic, as this will depend on such things as storm history, potential site evolution (soil accumulation) and vegetation dynamics.

Because of its application in forest management, it would be desirable to have a term that explicitly reflects possible changes in root strength contribution to slope stability. Building upon earlier development of the SHALSTAB theory, Dietrich et al. [1995] proposed an infinite slope model that includes the effects of vertical root strength and of vertical varying saturated conductivity. They couple a steady state hydrologic model with a infinite slope model in which soil cohesion, C_{sw} and apparent cohesion, C_r, due to root strength are included to derive a slope stability model that accounts for soil depth varia-

tion and effects of decreasing saturated conductivity with depth below the surface:

$$\frac{q}{k_1} = \frac{b \sin\theta}{a n_1}(e^{-n_1 \beta z \cos\theta} - e^{-n_1 z_0 \cos\theta} + \frac{k_2 n_1}{n_2 k_1} e^{-n_2 z_0 \cos\theta}) \quad (9)$$

where

$$\beta = 1 - \frac{\rho_s}{\rho_w}(1 - \frac{1}{\tan\phi}(\tan\theta - \frac{C_r + C_{sw}}{z \rho_s g \cos^2\theta})) \quad (10)$$

The saturated conductivity field is assumed to be described by an exponential decline in which the slope (n_1,n_2) and intercept (k_1,k_2) may change at a depth, z_0, due to changes in soil bulk density or transition to the underlying bedrock. All terms are the same as used in previous equations with the addition of C_{sw} and C_r, which are the soil cohesion and the apparent cohesion due to roots, respectively. With the use of an exponential decline in saturated conductivity, the hydrologic model is very similar to TOPMODEL [Beven and Kirkby, 1979]. Equation (9) is dimensionless as k_1 is the saturated conductivity at the ground surface and has the same units as the effective precipitation. Clearly, equation (10) requires much more information about site conditions that does SHALSTAB.

To model the soil depth influence on slope stability, Dietrich et al. [1995] also proposed a process-based theory for predicting the spatial pattern of soil depth. It is based on the assumptions that the rate of soil production varies inversely with soil thickness and that soil is redistributed across hillslopes by a linear diffusive transport model. Subsequently, the soil production assumption has been verified through cosmogenic radionuclide analysis [Heimsath et al., 1997], while Roering et al. [1999] have argued that the linear diffusion assumption may only apply on modestly inclined hillslopes. This modeling approach to including soil depth in slope stability analysis overcomes the challenging problem of mapping the soil depth, but it undoubtedly oversimplifies the actual pattern of depth variability across the landscape [Schmidt, 1999].

Most digital terrain based models use the assumption that soil depth is spatially constant in order to perform calculations [e.g. Okimura and Kawatani, 1987; Duan, 1996; Wu and Sidle, 1995; Pack et al., 1998] but this assumption greatly reduces the distinctive role of cohesion on slope stability. A modified version of SHALSTAB can illustrate this point. If all the same assumptions are made that led to SHALSTAB but in addition it is assumed that vertical root cohesion contributes to strength, then the slope stability equation can be written as:

$$\frac{q}{T} = \frac{b}{a \sin\theta}\left[\frac{\rho_s}{\rho_w}(1 - (1 - \frac{C_r}{\rho_s g z \sin\theta\cos\theta})\frac{\tan\theta}{\tan\phi})\right] \quad (11)$$

This form of the slope stability equations has been referred to as SHALSTAB.C [Dietrich and Montgomery, 1998)] and has been used in various analyses by Montgomery et al. [1998a,b; 2000] in which field estimates of cohesion and friction angle were used. If the ratio ($C_r/\rho_s g z$) = C^*, (11) becomes

$$\frac{q}{T} = \frac{b}{a \sin\theta}\left[\frac{\rho_s}{\rho_w}(1 - (1 - \frac{C^*}{\sin\theta\cos\theta})\frac{\tan\theta}{\tan\phi})\right] \quad (12)$$

If C^* is treated as a spatial constant, (12) differs little from SHALSTAB which does not have a cohesion term. To illustrate this point, we assume (12) and (7a) produce the same q/T for failure, then by setting (12) equal to (7a) and solving for friction angle in SHALSTAB yields

$$\tan\phi = \frac{\tan\phi_c}{(1 - \frac{C^*}{\sin\theta\cos\theta})} \quad (13)$$

in which $\tan\phi_c$ is the friction angle for the case with cohesion in (12) (whereas $\tan\phi$ is for the cohesionless case). The product $\sin\theta\cos\theta$ only varies from about 0.3 to 0.5 for 20 to 45 degrees, respectively. Therefore, if the ratio of cohesion to the soil depth-bulk density product is a spatial constant then there is a friction angle in the cohesionless case (SHASTAB) that will produce similar results. Hence, adding the cohesion term provides relatively little additional information about the system and there is no unique solution of cohesion and friction angle to the slope stability problem. Such a model may be, nonetheless, useful in illuminating how change in root strength associated with land management effects relative slope stability [Wu, 1993].

Pack et al., [1998] have released a digital terrain program based on equation (12) on the World Wide Web (http://www.engineering.usu.edu/cee/faculty/dtarb/sinmap.htm). They call the program SINMAP and have provided a well designed ArcView interface for handling data, making maps, and performing calibration of (12). Pack et al. let q/T, cohesion (divided by soil depth and bulk density, i.e. C^*) and friction angle be variables. They have the user display their landslide data on a plot of a/b versus slope (like that shown in Figure 5) and then interactively pick the combination of C^*, q/T and friction angle that visually best fits the data (i.e. for the majority of mapped landslides plot in the a/b and slope field that is predicted to be unstable). Each landslide is assigned a unique value of a/b and slope: the problem of landslides being bigger than the grid size and therefore having variable values of these topographic factors is not addressed. SINMAP asks the user to identify

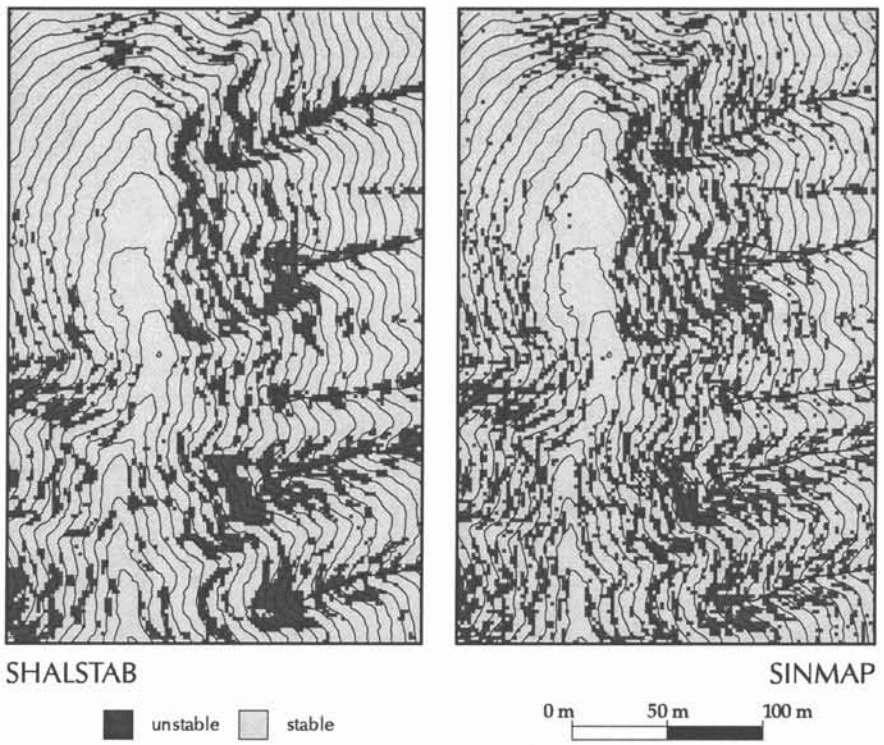

Figure 18. Comparison of predicted sites of instability using identical parameters (log(q/T) of -3.1, friction angle of 45 degrees, bulk density ratio of 1.6 and cohesion equal to zero) for SHALSTAB and for SINMAP. Site is a small portion of the Coos Bay study area. Contour interval is 5m and the thin lines in the valleys show the mapped channel location and the location of landslide scars.

upper and lower values of each of these three variables, and then assuming the values are normally distributed between these ranges and that the distribution functions are independent, the program calculates probability of failure. This probability is then used to assign a stability index to each site. The final product is a map of relative slope stability hazard based on assigned ranges of variables. While SINMAP is quite useful, it is not possible to uniquely determine cohesion (divided by bulk density and soil depth) and friction angle from data just on the location of landslides in a landscape unless the spatial variation in soil depth is also known. Even with that information, uniqueness is difficult to obtain [Dietrich et al., 1995]. It is also not clear how reliable the probability assignment is given the large uncertainty in parameter values and their covariance.

Differences between SHALSTAB, SINMAP, and other such digital terrain models may arise even if they use the same equations and parameters because the models may use difference procedures for estimating slope and drainage area. Tarboton [1997], for example, reports a detailed comparison between the performance of the algorithm for calculating area used in SINMAP and other methods including one called the multiple flow path procedure which is similar to that used in this paper. He argues in favor of his method because it is numerically efficient, and strikes a balance between highly directional and more dispersive flow paths. As mentioned earlier, we have chosen the multiple path procedure to minimize grid artifacts, i.e. we wanted to minimize results being dependent on the orientation of the topography relative to the grid. The SINMAP procedure is more sensitive to relative orientation than is the procedure we have used in SHALSTAB. In land use applications, it seems desirable to minimize orientation artifacts. We also use different procedures for estimating local slope. Figure 18 shows a comparison of the two programs for the same place with identical parameters. Three landslide scars are shown, and both models predict unstable cells where the scars are located. The more clustered appearance of the SHALSTAB model results from the dispersive area calculation procedure and the large area used to estimate local slope. This illustrates that details of

model predictions will depend on the specific methods used to calculate topography and users should be aware that such differences could occur.

CONCLUSION

The model SHALSTAB is a mechanistic, yet simple tool for delineating the relative potential for shallow landsliding using digital terrain models. This combination of being mechanistic and simple permits broad application in the absence of landslide maps or data on soil strength and hydrologic properties. Useful models that include root strength and dynamic runoff (non-steady flow) have been developed and provide insight about the land use and climatic controls on slope stability, but they are difficult to parameterize accurately across a landscape. We suggest further that because surface topography (local drainage area and slope) can have such a large effect on local slope stability that the most valuable information to improve model performance is increased topographic resolution. Even the best currently available 7.5' USGS quadrangles miss the fine scale topography that dictates local shallow subsurface flow paths. While validation studies support its use, they also show that the currently available topographic maps in the Pacific Northwest (7.5' USGS quadrangles) do not provide satisfactory topographic resolution to permit the application of site specific land use measures without field inspection. Hence, the digital terrain model can serve as a planning tool at the regional, watershed timber harvest level and as a guide for fieldwork when specific land use measures are being applied. Higher resolution topography, such as that obtained from laser altimetry, would greatly improve modeling and would have great utility in other land management activities (e.g. road design) and watershed analysis (e.g. mapping of channels, modeling wood recruitment to channels). These other applications could make it cost effective to obtain such higher quality topographic data.

Because this model can be used in a fixed parameter mode, a standard value of log(q/T) can be used to define high risk landslide areas. There remains the policy decision about what percentage of the observed landslides should be placed in the high risk class (i.e., what value of log(q/T) should be used to define the bound of high risk) and what should be the appropriate land use prescription for the relative stability classes. Plots of cumulative percentage of watershed area as a function of cumulative percentage number (or volume) of landslides associated with a log(q/T) threshold can be used to examine potential costs of choosing different threshold values. Restrictions should be greater where landslides could threaten structures and people. If we use the criteria that two-thirds of the mapped landslides (by volume) should fall in the high risk category, then for 10 m grid maps (used in this validation study), log(q/T) should be < -2.8 (placing on average 13% of the watershed area of our validation sites into high hazard). To obtain a similar level of performance we suggest a threshold of $\log(q/T) < -2.5$ for 30 m grid data and -3.1 for 5 m or less grid data. Digital maps can be gridded to any scale, so these grid scales refer to the original topographic data density from which maps are made. These log(q/T) thresholds are based on model performance, however, not on perceived environmental or economic risk. It is our view that uniform guidelines could be established in the absence of data using the model we have validated here, but that flexibility should remain in the field application in order to account for inaccuracies and to include the issue of risks to downstream resources as criteria for specific forest management decisions. Such combined use of digital terrain hazard mapping and field investigation should lead to the successful reduction in forest management related shallow landsliding even as active timber harvesting continues.

Acknowledgments. The development and testing of SHALSTAB reported here has been supported by Weyerhaeuser, Louisiana-Pacific, Mendocino Redwood Company, NCASI, Bureau of Land Management, Stillwater Sciences, and the Water Resources Center of the State of California. Landslide mapping of the Northern California watersheds was done by John Coyle. Martin Trso helped with data analysis. The Oregon Department of Forestry provided topographic data and maps of landslide locations and we specifically thank Jim Paul and Keith Mills. Conversations with many individuals including James McKean, Kathleen O. Sullivan, Thomas Spittler, Barry Williams, Bruce Orr, Mark Reid, and Frank Ligon were helpful. Reviews by John Stock, Josh Roering, Fred Booker, Douglas Allen, Mauro Casadei, Frank Ligon, and two anonymous readers improved the manuscript. Discussions with David Montgomery were, as always, valuable.

REFERENCES

Anderson, S. P., W. E. Dietrich, D. R. Montgomery, R. Torres, M. E. Conrad, and K. Loague, Subsurface flow paths in a steep unchanneled catchment, Water Resour. Res., 33, 2637-2653, 1997.

Anderson, S. A., W. E. Dietrich, R. Torres, D. R. Montgomery and K. M. Loague, Concentration-discharge relationships in runoff from a steep, unchanneled catchment, Water Resour. Res., v 33, 211-225,1997,

Benda, L, and T. Dunne, Stochastic forcing of sediment supply to channel networks from landsliding and debris flow, Water Resources Research, v. 33, p. 2849-2863, 1997.

Beven, K. and M. J. Kirkby, A physically based, variable contributing area model of basin hydrology, Hydrol. Sci. Bull., 24, 43-69, 1979.

Burroughs, E. R., Jr., and B. R. Thomas, Declining root strength in Douglas-Fir after felling as a factor in slope stability, U.S. Dept. of Agriculture, Forest Service Research Paper INT-190, 27p. 1977.

Burroughs, E. R., Jr., C. J. Hammond, G. D. Booth, Relative stability estimation for potential debris avalanche sites using field data, Internat. Symposium on erosion, debris flow and disaster prevention, 335-339, Tsukuba, Japan, 1985.

Carrara, A., Multivariate models for landslide hazard evaluation, Math. Geol., 15, 403-426, 1983.

Carrara, A., M. Cardinalli, F. Guzzeti and P. Reichenbach, GIS technology in mapping landslide hazard, in Geographical Information Systems in Assessing Natural Hazards, edited by A. Carrara and F. Guzzetti, pp. 135-175, Kluwer Academic Publishers, Netherlands, 1995.

Costa-Cabral, M. C., and S. J. Burges, Digital elevation model networks (DEMON): A model of flow over hillslopes for computation of contributing and dispersal areas, Water Resources Research, 30, 1681-1692, 1994.

Cutherbertson, J.G., Geotechnical evaluation of the slope stability computer program 3-D LISA, M.S. thesis, University of Idaho, Boise, 271p., 1992

Dietrich, W. E., and T. Dunne, Sediment budget for a small catchment in mountainous terrain, Zeit. für Geomorph., Suppl. 29, 191-206, 1978.

Dietrich, W. E., Dunne, T., Humphrey, N. F., and Reid, L. M., Construction of sediment budgets for drainage basins, in Sediment Budgets and Routing in Forested Drainage Basins, edited by F. J. Swanson, R. J. Janda, T. Dunne, and D. N. Swanston, General Technical Report PNW-141, Forest Service, U.S. Dept. of Agriculture, p. 5 - 23, 1982.

Dietrich, W. E., Wilson, C. J., Montgomery, D. R., McKean, J., and Bauer, R., Channelization thresholds and land surface morphology, Geology, v. 20, 675-679, 1992.

Dietrich, W. E., Wilson, C. J., Montgomery, D. R., McKean, J., Analysis of erosion thresholds, channel networks and landscape morphology using a digital terrain model, Journal of Geology, v. 101, 259-278, 1993.

Dietrich, W. E., R. Reiss, M.-L Hsu, and D. R. Montgomery, A process-based model for colluvial soil depth and shallow landsliding using digital elevation data, Hydrological Processes, v. 9, 383-400, 1995.

Dietrich, W. E., D. R. Montgomery, SHALSTAB: a digital terrain model for mapping shallow landslide potential, National Council of the Paper Industry for Air and Stream Improvement, Technical Report, 26p., 1998.

Dietrich, W. E., R. Real de Asua, J. Coyle, B. Orr, M. Trso, A validation study of the shallow slope stability model, SHALSTAB, in forested lands of Northern California, project report to Louisiana-Pacific Corporation, June 1998, 16p.

Dietrich, W. E. and N.Sitar, Geoscience and geotechnical engineering aspects of debris-flow hazard assessment, in Debris flow hazard mitigation: mechanics, prediction, and assessment, in C. Chen (edt), American Society of Civil Engineers, p. 656-676, 1997.

Duan, J., A coupled hydrologic-geomorphic model for evaluating effects of vegetation change on watersheds, unpublished Ph.D. dissertation, Oregon State University, 133p., 1996.

Dunne, T., 1991, Stochastic aspects of the relations between climate, hydrology and landform evolution, Trans., Japanese Geomorphological Union 12, 1-24.

Ellen, S. D., S. H. Cannon, S. Reneau, Distribution of debris flows in Marin County, in, Landslides, floods, and marine effects of the storm of January 3-5, 1982, in the San Francisco Bay Region, California, Ellen, S. D. and G. F. Wieczorek, 113-131, 1988

Endo, T., and T. Tsuruta, The effects of tree roots on the shearing strength of soil, Annual Report, Forest Experiment Station, Hokkaido, 167-182, 1969.

Fannin, R. J., M. P. Wise, J. M. T. Wilkinson, B. Thomson, E. D. Hetherington, Debris flow assessment in British Columbia, in Debris flow hazard mitigation: mechanics, prediction, and assessment, in C. Chen (edt), American Society of Civil Engineers, 197-206, 1997

Gray, D. H., and W. F. Megahan, Forest vegetation removal and slope stability in the Idaho Batholith, Res. Pap. INT-271, Forest Service, U.S. Dept. of Agriculture, Ogden, UT, 23pp., 1981.

Hammond, C., D. E. Hall, S. MIller, and P. Swetik, Level I stability analysis (LISA) documentation for version 2.0, U.S. Dept. of Agric. Forest Service, Intermount. Res. Sta., Gen. Tehcn. Rep. INT-285, Ogden, UT, 190p.

Heimsath, A. M., W. E. Dietrich, K. Nishiizumi, and R. C. Finkel, The soil production function and landscape equilibrium, Nature 388, 358-361, 1997.

Heimsath, A. M., W. E. Dietrich, K Nishiizumi, R. C. Finkel, Cosmogenic nuclides, topography, and the spatial variation of soil depth, Geomorphology, 27, 151-172, 1999..

Hsu, M., A grid-based model for predicting soil-depth and shallow landslides, unpublished Ph.D. dissertation, University of California, Berkeley, 253p., 1994.

Koler, T. E., Evaluating slope stability in forest uplands with deterministic and probabilistic models, Environ. and Eng. Geoscience, IV, 185-194., 1998.

Johnson, K. A. and N. Sitar, Hydrologic conditions leading to debris flow initiation, Can. Geotechn. J., 27(6), p. 789-801, 1990.

Martin, K., Forest management on landslide prone sites: the effectiveness of headwall leave areas and evaluation of two headwall risk rating methods, M.S. thesis, Oregon State University, Corvallis, 93p., 1997.

Montgomery, D. R., W. E. Dietrich, R. Torres, S. P. Anderson and J. T. Heffner, Hydrologic response of a steep unchanneled valley to natural and applied rainfall, Water Resources Research, 33, 91-109, 1997.

Montgomery, D. R., and W. E Dietrich, .A physically-based model for the topographic control on shallow landsliding, Water Resources Research, v. 30, 1153-1171, 1994.

Montgomery, D. R., W. E. Dietrich, and K. Sullivan, The Role of

GIS in Watershed Analysis, in Landform Monitoring, Modelling and Analysis, edited by S. Lane, K. Richard, and J. Chandler, John Wiley & Sons, pp. 241-261, 1998a.

Montgomery, D. R., K. Sullivan, and H. Greenberg, Regional test of a model for shallow landsliding, Hydrological Processes special issue on GIS in Hydrology, 12, 943-955, 1998b.

Montgomery, D. R., K.M. Schmidt, H. M. Greenberg and W. E. Dietrich, Forest clearing and regional landsliding, Geology, 28, 311-314, 2000.

Moore, I.D., E. M. O'Loughlin, and G. J. Burch, A contour-based topographic model for hydrological and ecological applications, Earth Surf. Process. Landforms, 13, 305-320. 1988.

Okimura, T., and R. Ichikawa, A prediction method for surface failures by movements of infiltrated water in a surface soil layer, Natural Disaster Science, 7, 41-51, 1985.

Okimura, T. and T. Kawatani, Mapping of the potential surface-failure sites on granite mountain slopes, in International Geomorphology 1986, Part I, V. Gardiner (edt.), J. Wiley and Sons, 121-138, 1987.

Okimura, T. Prediction of slope failure using the estimated depth of the potential failure layer, Jour. Natural Disaster Sci., 11, 67-79, 1989.

Okimura, T., and M. Nakagawa, A method for predicting surface mountain slope failure with a digital landform model, Shin-Sabo, v. 41, 48-56, 1988.

Okimura, T. Prediction of the shape of a shallow failure on a mountain slope: the three-dimensional multi-planar sliding surface method, Geomorphology, 9 , 223- 233, 1994.

O'Loughlin, E. M., Prediction of surface saturation zones in natural catchments by topographic analysis: Water Resour. Res., 22, 794-804, 1986.

Olson, C.M. and B.K. Orr., Combining tree growth, fish and wildlife habitat, mass wasting, sedimentation, and hydrologic models in decision analysis and long-term forest land planning. Forest Ecology and Management, 114, 339-348, 1999.

Pack, R. T. and D. G. Tarboton, New developments in terrain stability mapping in B.C., Proc. of the 11th Vancouver Geotechnical Soc. Symp- Forestry Geotechnique and Resource Engineer., 12p., 1997.

Pack, R.T., D. G. Tarboton, and C. N. Goodwin, SINMAP: a stability index approach to terrain stability hazard mapping, available at http://www.engineering.usu.edu/cee/faculty/dtarb/sinmap.htm , 1998.

Pierson, T. C., Factors controlling debris-flow initiation on forested hillslopes in the Oregon Coast Range, unpublished Ph.D., University of Washington, 166p., 1977.

Prellwitz, R. W., A complete three-level approach for analyzing landslides on forest lands, in Proceedings of a workshop on slope stability: problems and solutions in forest management, U.S. Dept. of Agric. For. Serv. Pac. Northwest, Res. Sta., Gen. Tech. Report PNW-180, 94-98, 1985.

Quinn, P., K. Beven, P. Chevalier and O. Planchon, The prediction of hillslope flow paths for distributed hydrological modelling using digital terrain models. Hydrol. Proc., 5, 59-79, 1991.

Reeves, G.H., L.E. Benda, K.M. Burneet, P. A. Bisson,and J. R. Sedell, A disturbance-based ecosystem approach to maintaining and restoring freshwater habitats of evolutionary significant units of anadromous salmonids in the Pacific Northwest, Symp. Evolution and the Aquatic System: Defining Unique Units in Population Conservation, Am. Fish. Soc. 17, 334-349, 1995.

Reneau, S. L., W. E. Dietrich, C. J. Wilson, and J. D. Rogers, Colluvial deposits and associated landslides in the northern San Francisco Bay area, California, USA: *in* Proceedings of IVth International Symposium on Landslides, International Society for Soil Mechanics and Foundation Engineering, Toronto, Canada, p. 425-430, 1984.

Reneau, S. L., and W. E. Dietrich, Size and location of colluvial landslides in a steep forested landscape, in Erosion and Sedimentation in the Pacific Rim, edited by R. L. Beschta, T. Blinn, G. E. Grant, F. J. Swanson, and G. G. Ice, Int. Assoc. Hyd. Sci. Pub. 165, 39-49, 1987.

Reneau, S. L., and W. E. Dietrich, Depositional history of hollows on steep hillslopes, coastal Oregon and Washington, National Geogr. Res., 6, 220-230, 1990.

Roering, J J., J. W. Kirchner, and W. E. Dietrich, Evidence for non-linear, diffusive sediment transport on hillslopes and implications for landscape morphology, Water Resour Res, 35, 853-870, 1999.

Rollerson, T. P., B. Thomson, T.H. Millard, Identification of Coastal British Columbia terrain susceptible to debris flows in Debris flow hazard mitigation: mechanics, prediction, and assessment, in C. Chen (edt), American Society of Civil Engineers, 484-495, 1997

Schroeder, W. L., and J. V. Alto, Soil properties for slope stability analysis; Oregon and Washington coastal mountains, Forest Sci., 29, 823-833, 1983.

Sidle, R. C., A. J. Pearce, C. L. O'Loughlin, Hillslope stability and land use, Amer. Geophy. Union, Wat. Res. Mon. 11, 140p., 1984.

Sidle, R. C., A theoretical model of the effects of timber harvesting on slope stability, Water Resour. Res., 28, 1897-1910, 1992.

Swanson, F. J. and C. J. Roach, Administrative report, Mapleton leave area study, USDA Forest Service, Pacific Northwest Res. Sta., Corvalis, Oregon, 139p., 1987.

Tang, S. M., and D. R. Montgomery, Riparian buffers and potentially unstable ground, Environmental Management, 19, 741-749, 1995.

Tarboton, D. G., A new method for the determination of flow directions and upslope areas in grid digital elevation models, Water Resources Research, 33, 309-319, 1997.

Torres, R., W. E. Dietrich, D. R. Montgomery, K. Loague , and S. P. Anderson,, Unsaturated zone processes and the hydrologic response of a steep, unchanneled catchment, Water Resour.Res., v. 34, p.-1865-1879, 1998.

Ward, T.H., R. Li, and D. B. Simons, Mapping landslide hazards in forest watersheds, J. Geotech. Engin., Am. Soc. Civil Engin. 108, 319-324, 1982.

Wieczorek, G.F., G. Mandrone, L. Decola, The influence of hillslope shape on debris-flow initiation, in Debris flow hazard mitigation: mechanics, prediction, and assessment, in C. Chen (ed.), American Society of Civil Engineers, 21-31, 1997.

WFPB (Washington Forest Practices Board), Board manual: Standard methodology for conducting watershed analysis under Chapter 222-22 of the Washington Administrative Code (WAC), Versioni 4.0, Washington Department of Natural Resources, 1997.

Wu, W., Distributed slope stability analysis in steep, forested basins, Ph.D. thesis, Utah State University, 134p., 1993

Wu, W., and R. C., Sidle, A distributed slope stability model for steep forested basins, Water Resour. Res., 31, 2097-2110, 1995.

Zhang, W., and D. R. Montgomery, Digital elevation model grid size, landscape representation, and hydrologic simulations, Water Resources Research, 30, 1019-1028, 1994.